Effects of Surface and Molecular Shape on Liquid Crystalline Ordering and Phase Transition

Toshikuni Miyazaki*

Keywords: Liquid crystal, Molecular dynamics, Phase transition, Gay-Berne model, Surface stabilised ordering, Molecular bend

1. Introduction

An appearance of liquid crystalline phase is due to an anisotropic interaction, which comes from elongated shape of constituent molecules. So, the relation between the molecular shape and liquid crystalline order is an interesting problem. On the other hand, the ordering in the confined system is quite important problem, because in the application of liquid crystal to the display liquid crystalline materials are put between parallel walls, where the ordering is affected strongly by the boundary walls due to a softness of the order. In this work the effects of surface together with the molecular shape on liquid crystalline ordering and phase transition are studied by molecular dynamics simulation.

In the first half of the paper, the system composed of Gay-Berne molecules in the sandwiched cell is tested, where various types of wall conditions are tested. We have elucidated that a new type of smectic phase appears because of the effect of walls on both direction and smectic layer. In the latter half, two types of molecules are introduced to clarify the relation of molecular shape to the ordering and phase transition; one is composed of realistic molecules based on the molecular orbital calculation (MO) and the other is of bend Gay-Berne molecules.

2. Effect of walls on liquid crystalline ordering and phase transition in the thin systems

Constant temperature, constant volume molecular dynamics simulation (NTV-MD) at the system of Gay-Berne model is carried out to study the effects of walls on the orientational order and positional smectic one. The walls in the top and bottom of the simulation box are replaced by imaged particles which interact with Gay-Berne molecules showing various anchoring forces. The system exhibits several phases successively, an isotropic, nematic, smectic and crystalline phases as the temperature is decreased, in which the clearing temperature is higher than that at bulk system. In the case of homogeneous anchoring condition, surface-stabilised smectic phase (SmAII) is shown to appear in the lower temperature side of the usual smectic A phase (SmAI) and phase transition between them is certified. Degrees of the positional and orientational orders

of the former are higher than those of the latter. These results indicate that the wall works not only as the field

* Toyotatechnoservice Corporation

to enhance the orientational order but also as a symmetry breaking field inducing the smectic layer order in case the thickness of the system is smaller than a healing length. The appearance of two kinds smectic phases is analysed by generalising McMillan theory and it is confirmed that the effect of wall works as the symmetry breaking field applied to molecules neighbouring to the walls.

As an analogue of the Freedericksz transition at nematic phase, a response to the transverse electric field at SmAII is studied by NTV-MD to certify a stability of SmAII. At a threshold value of the field strength, the system changes to SmAI with layer normal parallel to the electric field via an intermediate phase like a smectic C phase. By reducing the field strength, again SmAII appears directly, showing a hysteresis characteristic to a discontinuous transition. The dipole-dipole interaction is proved to stabilise the layer structure of smectics, while SmAI changes to smectic C phase in the electric field.

3. Effects of molecular shape on liquid crystalline ordering and phase transition

In two types of model systems, MD simulations are carried out to study the effect of molecular shape on the ordering and phase transition of liquid crystals. In one case, a realistic molecule is constructed by MO in vacuum, and the system is composed of about 100 molecules in the simulation box. Inter-atomic interactions between different molecules are given by a type of Lennard-Jones potential, while molecular deformations in shape are described in terms of harmonic springs. This system is studied by the constant temperature pressure molecular dynamics (NTP-MD) to elucidate ordering and switching of antiferroelectric smectic phase. The bending angle of the chiral chain as well as the angle of achiral one is shown to be enhanced compared with those at isolated state. Tilt angle agrees well with the experimental one. A response at an anticlinic alignment to the transverse electric field is also tested.

In the other case, NTV-MD of polar bend molecules is carried out to study the relation between the molecular shape and dipole moment to the ordering and polarisation of liquid crystal. The molecule of this system is a dimer of Gay-Berne particles coupled by a harmonic spring at each end making bend angle, and a permanent dipole is attached to it. The appearance of the polarisation together with biaxiality is tested for various combinations of position and direction of the dipole. A decrease of clearing temperature with an increase of the bend angle is depicted. By changing hardness of the spring, the clearing temperature shows sigmoidal curve and nematic phase is hardly observed in the soft limit. The electric polarisation is observed exclusively in the system of molecules where the dipole is attached in a direction perpendicular to the molecular long axis at the connecting point. Biaxiality occurs accompanying the polarisation.

A Study of New Polymerization Suppressors for Common Monomers

Jun-ichi Nakajima†
(Organic Chemistry for Material, Division of Material Science)

Keywords:, Polymerization suppressor, Polymerization inhibitor, Polymerization retarder, Dodecylbenzenesulfonic acid, Triplet carbenes, Laser Flash Photolysis

It is well known that unsaturated monomers undesirably polymerize at various stages of their manufacture, processing, handling, storage, and use. The polymerization during their purification results in the loss of the monomer and a loss in production efficiency owing to the deposition of polymer in or on the equipment used in the purification. A wide variety of compounds have been proposed and used for inhibiting undesired polymerization of monomers. For styrene, which is one of the most important monomer, dinitrophenols have been commercially used as in-process retarder. However dinitrophenols are extremely toxic and highly reactive and hence special precaution is required for their use. The present study was undertaken to elucidate the mechanism of inhibition and retardation of thermal polymerization of styrene by dinitrophenols and also to develop a new retarder which can be used as an alternative to dinitrophenols.

The previous reports concerning inhibition of the polymerization and commercial styrene manufacturing process are first outlined. Several features of dinitropnenols are also mentioned.

In order to elucidate mechanism of dinitrophenols retardation against thermal radical polymerization of styrene, the effects of nitrophenols structure on the rate of nitorophenols consumption in the thermal polymerization of styrene and on the molecular weights of polystyrene formed were examined. The result suggested that the efficiency of the retardation depended on structure of phenolic hydroxyl group and discussed in terms of the relationship between stability of nitrophenolic radicals generated by hydrogen abstraction during propagation radical and the retardation performance of nitrophenols.

It was found that dodecylbenzenesulfonic acid (DBS) reduced the initial rate of thermal radical polymerization of styrene. In order to know the origin of DBS retardation, product analysis and molecular weight of polystyrene were conducted. The results showed that, unlike most of inhibitors and retarders, DBS did not act as a hydrogen donor but behaved as an acid catalyst for the isomerization of initial Diels-Alder dimmer of styrene, which is known to act as a radical precursor for polymerization, to 1-phenyltetralin. The efficiency of DBS on retardation of thermal polymerization was found to be lower compared with that of dinitrophenols but it can be used to reduce the amount of dinitrophenols required in the styrene distillation process. The field test in commercial styrene manufacturing plant were also performed.

Tetramethylpiperidine-1-oxyls (TEMPOs) are excellent trapping regents for carbon centered radicals and are known as a useful inhibitor for several kinds of monomers. However, for auto-polymerization of styrene, TEMPOs were found to show unique behavior. For example TEMPOs were consumed not only by quenching styrenic radical but also by attacking styrene monomer or the radical precursor. The mechanism for TEMPOs consumption in styrene polymerization was discussed.

To estimate TEMPOs performance as polymerization inhibitor, TEMPOs reactivity towards triplet carbenes was studied. The absolute rate constants for the quenching reaction were measured by means of a laser flash photolysis technique. The result showed that the reactivity of TEMPOs towards triplet carbenes was lower than that of oxygen but higher than that of 1,4-cyclohexadiene. TEMPOs are shown to be very convenient regents to estimate the reactivity of triplet carbenes.

†Hakuto Co., Ltd

A Study on Environmental Education Facility Planning for Promoting Environmental Conservation Bodies

Hiroki Ogawa
(Architecture and Planning, Division of System Engineering)

Keywords: Environmental Education Facility, Learning Program, Environmental Conservation Body

1. The Purpose

The purpose of this study is to clarify a condition of learning programs (software) and environmental education facilities (hardware) for promoting environmental conservation bodies. In other words I clarify the present conditions of learning programs and environmental education facilities corresponding from personal upbringing to organization upbringing. And, through analysis of the structure promoting them continually, I clarify environmental education facility planning.

2. The Present Conditions of Learning Programs and Environmental Education Facilities

Environmental education should be carried out step by step: first is Awareness, second is Understanding, and third is Participation. This paper analyzes the effects of the phased environmental education programs, by carrying out a questionnaire to investigate the education programs of 213 environmental education facilities. Findings are as follows: Less than half of the environmental education facilities implement a continuous phased environmental education programs. However, the programs can promote class members to participate in projects or programs of these facilities, and to form new organizations to manage local environments.

3. Characteristics of the Learning Room from the Viewpoint of Aim Stage on Learning Programs

This clarifies the relation between learning rooms and learning programs of environmental education facilities. Main results are as follow: There are many learning programs of interest or knowledge stage, and a few one of action or understanding stage. Many facilities carry out programs of the only interest stage. But more than half execute learning programs that have a combination of some aim stages. From the equipments of learning room, the use form of learning room is classified in lecture, training, teaching materials, and exhibition. Learning programs of using the plural room are able to achieve a higher stage than ones of the single room use.

4. The Planning and the Evaluation of Talented People Raising Program

In environmental learning, talented people training programs are important to assure an action to treat environmental problems, and the follow-up programs are too. The Mie environmental education seminar is planned and evaluated program from viewpoint of PDCA cycle as an example. We comprehended the achievement degree of this seminar's aim by investigation of students who attended this program, and let follow-up programs reflect it. As a result, it led to improvement of environmental consciousness and action of students. Learning continued by giving an opportunity of follow-up programs. And a change more was seen in environmental consciousness and action of students. To stimulate such a change, the follow-up programs to become a leader or to utilize knowledge or skill that they learned was effective.

5. Support Demand of Environmental Conservation Bodies and Facility Correspondence for it

Though many supports for citizen organizations concerned with the environment preservation are provided, there is a gap between support programs and the needs of citizen organizations. To make a cause of the gap clear, a

questionnaire of 250-citizen organizations in Mie prefecture was carried out. The results are as follows; citizen organizations are classified 4 types, and each type has different support needs. Therefore the support programs should be necessary to be produced according to the needs of citizen organizations. And intermediate support organizations should meet needs of citizen organizations and support programs.

6. Conclusions

From this study, I got the following conclusion. :

1) The conditions of learning program
  a. Structure corresponding from personal upbringing to organization upbringing
  b. Carry out the learning programs combined a theory and practice on personal upbringing
  c. Carry out the follow-up programs on organization upbringing
  d. Participate in making learning programs with an early organization
2) The conditions of environmental education Facility
  a. Make the special facilities
  b. Get the room ready to learning programs with aim stage
  c. Get the room ready to use organization activity

Furthermore, as a future problem, I want to clarify about cooperation of specialized facilities and associated ones.

Flash Welding Control by Use of PWM Inverter Power Supply

Yukihiko Sato
(Power Electronics, Division of System Engineering)

Keywords: Flash welding, Inverter control, PWM inverter power supply, Flashing control

1. Introduction

Flash welding has several advantages in spite of open air welding. One is materials with heavy cross section can be welded in a short time. Other is easy to obtain high quality of weld joints. It is well known that it is important to keep flashing continuous for high quality of weld joints. To achieve continuous flashing, mechanical control combined with electro hydraulic valve and hydraulic cylinder has been applied. However, as mechanical flashing control has a limit of response for more precise control, an application of power electronics, especially, PWM inverter is discussed for flash welding control.

2. Purpose

Flashing phenomena control strategy for flash welding is proposed by use of PWM inverter power supply in this paper.

3. Results

Since no study has been reported regarding flashing phenomena using square wave alternating current, flashing phenomena in 100Hz square wave alternating current using PWM inverter power supply are analyzed for flashing control. The analyzed results give a suggestion that PWM inverter has possibility to control flashing phenomena such as number of flashing pulses or degree of resistance heating by changing the modulation factor of PWM inverter. Based on the analyzed results, an inverter control method named " full power control method " is proposed for continuous flashing. The concept of the proposed inverter control method is different from a conventional feedback PI control. In the control system, the inverter supplies the maximum output by changing modulation factor of PWM inverter when detecting current is over the reference value. When the current is under the reference value, inverter supplies the original output. The test results show that the proposed inverter control method makes it possible to get the reqired number of flashing pulses in half a cycle, and the control is useful for continuous flashing. The results also show that the control method enables to control degree of resistance heating. The resistance heating method with a few flashing is proposed for resistance heating. Finally, PWM inverter control method for flash process in flash welding is proposed using the " full power control method ". In the control system, welding starts with a few flashing pulses and finally the number of flashing pulses are increased up to maximum. The feature of this control is that local contact bridges are maintained during flash process, and the number of flashing pulses are controlled by changing modulation factor of PWM inverter up to maximum.

4 Conclusion

It has been known that it is impossible to control flashing phenomena, especially, the number of flashing pulses at any time. This paper has shown that an application of PWM inverter makes it possible to control flashing phenomena.

Study on Optical Properties and Application of Nano-Sized Silver Particles Prepared by the Evaporation-Condensation Method

Noritsugu HASHIMOTO †

Key words: Nano-Sized Silver Particle, Localized Surface Plasmon Resonance, Optical Nonlinearity, Optical Sensor, Evaporation-Condensation Method, Sol-Gel Method

1. Introduction

Nano-sized silver particles are expected to be applied to nonlinear optics devices because of their large nonlinear susceptibility and fast response time. In addition, it is well known that silver nanoparticles exhibit a unique optical absorption in the visible light region due to localized surface plasmon resonance (LSPR), which may be applicable to optical sensors. In this thesis, the formation process of nanoparticles, and nonlinear and/or linear optical properties of nano-sized silver particles prepared by the evaporation-condensation method were concerned, and their applicability to optical sensor based on LSPR, so-called SPR sensor, was examined.

2. Bipolar charging and neutralization of nano-sized aerosol particles

The formation of silver particles through the evaporation-condensation process, and charging and neutralization probabilities for the particle size fractioning were discussed. The charging probability by Am-241 for aerosol particles of larger than 3 nm was in good agreement with one theoretically predicted by Fuchs, while in the case of those smaller than 3 nm such an agreement was not achieved.

3. Preparation of silver films consisting of nano-sized silver particles by the evaporation-condensation method, and their linear and nonlinear optical properties

The preparation of films consisting of nano-sized silver particles on the silica glass substrate, and their linear and nonlinear optical properties were examined. Film samples were prepared by depositing silver particles generated by the evaporation-condensation method on the silica glass substrates.

Silver particles deposited on the silica glass substrate exhibited an optical absorption peak due to LSPR, which shifted toward longer wavelength side with increasing the particle generation temperature, or with the increase of the particle diameter. On the contrary, when annealed at 170 °C, the absorption peak was shifted drastically to shorter wavelength as 410 nm, independently of the particle generation temperature. Nonlinear optical properties (nonlinear refractive index, γ, and nonlinear absorption coefficient, β) were determined by *Z*-scan technique. Figure 1 shows the size dependence of γ for silver particles deposited on the silica glass substrate. It was found that γ and β of silver nanoparticles were negative, and the absolute value of γ was increased with inverse of d^3 as has been theoretically predicted.

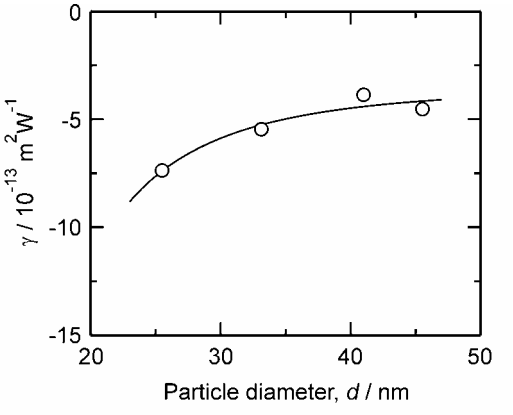

Fig. 1. Size dependence of γ for silver particles deposited on the silica glass substrate, and annealed at 170 °C.

The changes of surface morphology and optical properties of silver particles deposited on the silica glass substrate or sol-gel

† Ceramics Laboratory, Industrial Research Division, Mie Science and Technology Promotion Center

derived silica film upon annealing at temperatures from 100 to 500 °C were examined. When the silver film was annealed at above 200 °C, the dense packing of silver particles was disrupted and the surface morphology of the film turned to be island-like, accompanying with the absorption peak shift toward shorter wavelength.

4. Application of nano-sized silver particles to optical sensor based on LSPR

The new type of SPR sensor was proposed as an application of nano-sized silver particles. The silica glass dispersed with silver particles was prepared by the sol-gel method (film (a)). The sensor films were also prepared by depositing silver particles on the silica glass substrates (film (b)) or on sol-gel derived silica films (film (c)). For evaluating the sensor characteristics, the LSPR absorption peak wavelength was measured in various liquids having different refractive indices, *n*. The sensitivity was defined as the absorption peak shift with the change of *n*, i.e., dλ/d*n*. Figure 2 shows the relationship between LSPR absorption peak wavelength and refractive index of immersion liquid. The LSPR absorption peak wavelength for the film (a) showed scarce change with *n* of the liquid. While, that of Films (b) and (c) changed linearly with *n*. This fact indicates that latter films are applicable to the SPR sensor. The sensitivity was largest as 111.8 nm for film (c), which may be attributable to the fact that silver particles was stuck in the soft film and their growth was suppressed during the deposition.

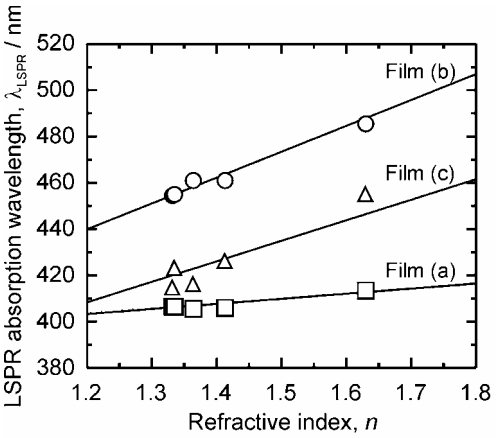

Fig. 2. Relationship between LSPR absorption peak wavelength and refractive index of immersion liquid.

In order to avoid the deterioration of the absorbance of the silver particle/silica film sensor during repeated applications, silver particles were overcoated with thin silica film prepared by sonogel method, and cycle performance was examined. Cycle performance was defined as the change of absorbance, *A*, with the cycle number, *N*, i.e., d*A*/d*N*. The relationship between absorbance at peak position and cycle number for silver particles-deposited silica glass with the overcoating is shown in Fig. 3. The d*A*/d*N* was decreased with increasing the thickness of overcoated film, while the sensitivity was still high as 59.4 nm. This fact means that the sono-silica overcoating of the composite sensor film is useful to improve cycle performance.

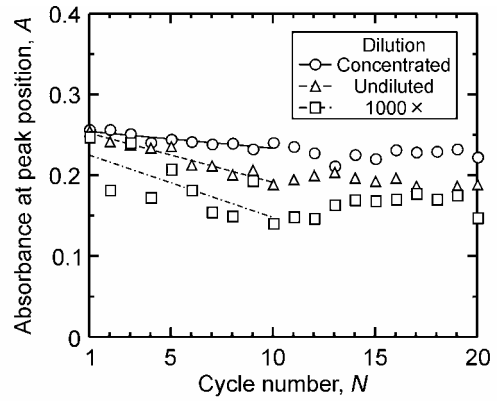

Fig. 3. Relationship between absorbance at peak position and cycle number for the sensor film.

5. Concluding remarks

The silver film consisting of nano-sized silver particles was successfully prepared by the evaporation-condensation method, and their nonlinear optical properties were determined. It was found that the γ and β of silver film were negative, and the size dependence of γ on the particle diameter as has theoretically predicted was experimentally observed. In addition, the applicability of nano-sized silver particles to SPR sensor was examined. As a result, the sensitivity of silver particles deposited on sol-gel derived silica glass substrate was high as 111.8 nm. In addition, the deposition of thin silica film on silver particles as the overcoating improved cycle performance of SPR sensor successfully.

Author's Publications

[1] M. Alonso, Y. Kousaka, T. Nomura, N. Hashimoto and T. Hashimoto, *J. Aerosol Sci.*, **28** (1997) 1479–1490.

[2] N. Hashimoto, T. Hashimoto, H. Nasu and K. Kamiya, *J. Ceram. Soc. Japan*, **112** (2004) 204–209.

[3] N. Hashimoto, T. Hashimoto, K. Mori, H. Nasu and K. Kamiya, *J. Ceram. Soc. Japan*, **112** (2004) S576–S578.

[4] N. Hashimoto, T. Hashimoto, T. Teranishi, H. Nasu and K. Kamiya, *Sens. Actuators, B*, in press.

[5] N. Hashimoto, Y. Yamamoto and S. Niijima, *e-J. Surf. Sci. Nanotech.*, **3** (2005) 120–124.

Development research of the novel methotrexate derivatives for treatment of an antirheumatic agent

Noriaki Maruyama[†]

(Materials Chemistry, Division of Materials Science)

Keywords: Antirheumatic Agent, Methotrexate, MX-68, Original route, Imprved route, large-scale preparation.

1. Introduction

MX-68, which is a novel methotrexate (MTX) derivative, has exhibited potent antirheumatic activity both *in vitro* and *in vivo* tests. Therefore, to supply sufficient quantities required for both the toxicity test and the clinical study, it was imperative to develop a large-scale preparation route.

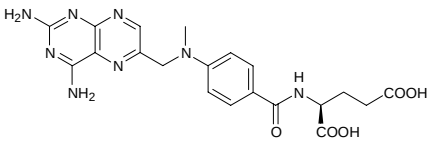

MTX (1)

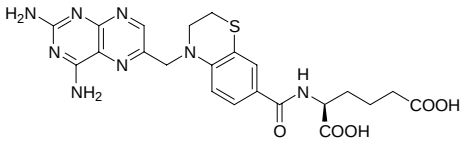

MX-68 (2)

An original route for structure-activity relationship studies is presented in **Scheme 1**. This route, designed based on the standard synthesis of MTX derivatives, involved several problems for a large-scale preparation. For example, use of corrosive reagents, low yield at the deprotection step, purification by column chromatography using $CHCl_3$, and major impurity formation at the final step.

Herein, we would like to report a new route, which has been accomplished by improving the original process, specifically for a large-scale preparation of MX-68.

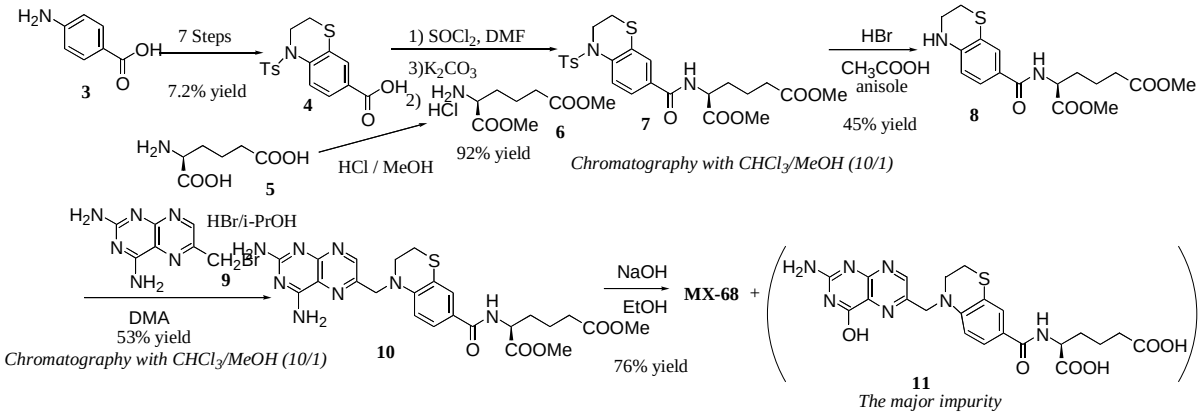

Scheme 1. Original route

2. Results and Discussion

We chose an improvement of the original route because the problems for the large-scale preparation were clear. Therefore, we focused on the solution of the problems by the following methods: change of the corrosive reagents to other reagents, replacement of the protected amine **4** to the unprotected amine **12**, change of the

[†] Synthetic Technology Research Dep., Pharmaceutical Technology Div., Chugai Pharmaceutical Co., Ltd.

chromatographic purification to crystallization, and improvement of the reaction condition at the final step to minimize the major impurity formation. Furthermore, these improvements were expected to lead to an increase in the total yield and provide a more environmentally friendly synthesis.

2-1. Alternative Preparation of the Amide 8.

In the original route, the amide **8** was obtained from the *N*-protected amine **7** by removing the *p*-toluenesulfonyl group but in low yield. The reason for the low yield was inferred from the simultaneous hydrolysis of the methyl ester groups in **7**, where the reaction was conducted under strong acidic conditions. Therefore, we carried out the coupling of the unprotected amine **12** with the diester **6** using several coupling reagents. As a result, using HOBt and WSC, **8** was obtained in the best yield.

Furthermore, in order to avoid use of saturated HCl, the corrosive reagent, was replaced with 2 equivalents of MsOH in the esterification of L-homoglutamic acid **5**. After the esterification was followed by neutralization with 2 equivalents of Et_3N, the reaction mixture was directly used in the subsequent coupling reaction. This new esterification process could avoid the use of the corrosive reagent, and at the same time shorten the operation time by eliminating the isolation process of the diester **6**.

2-2. Optimization of preparation of the diester 10.

In the original route, the amide **8** reacted with 2,4-diaminopteridine **9** in 16 times volume of DMA for 3 days at 70°C, extracted with $CHCl_3$, and the product was purified by silica-gel column chromatography using $CHCl_3$/MeOH (10/1) to give the diester **10** in 53% yield. In order to scale up this process, we tried to shorten the reaction time and to eliminate the chromatographic purification using $CHCl_3$, which was not suitable from an environmental standpoint. First, the amount of the solvent was examined, where the amount of DMA was changed from 16 times volume into 5 times. As a result, the reaction could complete within 4 hours. Next, the work-up procedure was examined in order to avoid using $CHCl_3$ and the chromatographic purification, As a result, the 3 times of recrystallization from MeOH/water to give **10** in 56 % yield in pure form.

2-3. Improvement of the reaction condition at the final step.

The major impurity obtained from this reaction was the by-product **11**, which had a hydroxyl group instead of the 4-amino group on 2,4-diaminopteridine moiety. **11** was difficult to remove from MX-68. In order to minimize the formation of **11**, several reaction conditions were studied using LiOH as a base. As a result, the reaction conducted at 0°C in acetonitrile / H_2O (10/15) was found to be the best way relative to both the impurities and the reaction time.

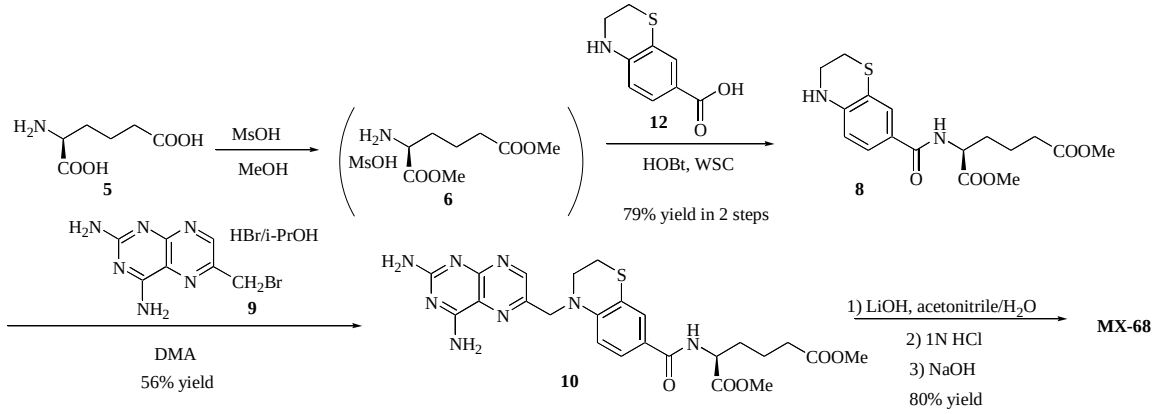

Scheme 2. Improved route of MX-68 for large-scale preparation

3. Conclusions

We have developed a large-scale preparation route of MX-68, presented in **scheme 2**, by improving the original route. Because the *N*-protected amine **4,** used in the original route as a starting material, was replaced with the unprotected amine **12**, the deprotection step using HBr/AcOH, a corrosive reagent, was eliminated. Therefore, the new route is suitable for a large-scale preparation. As a result of optimizing the reaction conditions and improving the isolation method of the compound **10,** no chromatographic purification was required for the coupling reaction of the amine **8** with the 2,4-diaminopteridine **9**. Furthermore, minimizing the formation of the major by-product **11** contaminating the final product of MX-68 was achieved by optimizing the hydrolysis conditions of the diester **10**. Thus, the present improved process provided us with MX-68 in overall yield of 37% from the unprotected amino acid **12**, and was able to supply sufficient quantities required for both the toxicity test and the clinical study of MX-68.

Auther's Publication

[1] Maruyama, Noriaki; Shimizu, Hirohito, Sugiyama, Takashi; Watanabe, Masashi; Makino, Masashi; Kato, Masahiro; Shimizu, Makoto, An Improved Process for the Large-scale Preparation of Antirheumatic Agent, MX-68. *Org. Process Research and Development*. **2004**, 8, 883-888.

[2] Maruyama, Noriaki; Shimizu, Hirohito, Sugiyama, Takashi; Watanabe, Masashi; Makino, Masashi; Kato, Masahiro, Process Development of MX-68: Anti Rheumatoid Arthritis Agent. The Japanese Society for Process Chemistry 2004 Summer Symposium abstracts 84-85.

Experimental Research on Mechanical Evaluation of Spinal Instability.

Takaya Katoh
(Bio System Engineering of Material Science)

Keywords : Biomechanics, Spinal instability, Mechanical evaluation, Experimental Research

1. Introduction

The role of the spine in the human body is supporting of trunk, transmission of movement through joint and muscle, and protection of spinal cord. These roles cannot be played due to the tissue destruction, breakdown of structural balance are caused by injury and congenital anomaly and tumor. Therefore it is very interesting to analyze the spine dynamically and to clarify the transforming behavior. It is thought that to investigate them becomes a help of the medical about the evaluation of the treatment policy, the surgical technique, and even the development of spinal instrumentation.

In the treatment of lumbar spinal diseases, the degree of lumbar spinal instability largely affects selection of treatment strategy and surgical technique. However, quantitative judge of lumbar spinal instability is very difficult, because the evaluation of lumbar spinal instability depends on surgeon's experience and feeling. In other words, evaluation of the lumbar spinal instability in the clinical spot is not performed objective and quantitative.

Currently, there are a few reports on the measuring instrument that can evaluate lumbar spinal instability during surgery. But, most of them are complicated and large-scale instrument. So they need motor, displacement measurement instrument and personal computer and more. Therefore, unfit for the clinical application, because they need long measuring time, installation space and cost.

2. Purpose

Purpose of this study is to seek easy method for measuring lumbar spinal instability, and to develop a practical intraoperative lumbar spinal instability measuring instrument. We performed basic experiment and clinical application for the development of instrument. Basic experiment was performed for to examine about relation of the degree of lumbar spinal instability and displacement between spinous processes about the cephalocaudal direction by using the human cadaveric lumbar spine.

3. Results and discussion of basic experiment

In the basic experiment, the relation of the force and displacement which are produced between spinous processes was investigated. The experiment method gave dilating force (20[N]) to the cephalocaudal direction using the machine of exclusive use and measured the displacement between spinous processes. Result of basic experiment is shown in Fig. 1. In the Fig. 1, horizontal axis is displacement between spinous processes and vertical axis is damage level (degree of lumbar spinal instability). As for these damage models, damage becomes large from [damage 1] to [damage 9]. It was found that the value of displacement of spinous processes stepwisely increased as severity of injury is increased in this graph. From this result, lumbar spinal instability was evaluated simply by displacement between spinous processes.

From result of basic experiment, we produced instrument that can generate dilating force and can measure displacement on cephalocaudal direction between spinous processes. The body of measuring instrument is hemostatic forceps with the push spring and the strain gauge (Fig. 2). Push spring is to generate dilating force. Furthermore strain gauge is to measure deformation of hemostatic forceps. The value of strain is reflect the balance of dilating force and displacement of spinous process. Next, we examined the relation of the degree of lumbar spinal instability and strain value of our instrument using human cadaveric lumbar spinal damage model. This model is the same as the above-mentioned model. The result is shown in Fig. 3. In the fig. 3, horizontal is strain value of instrument and vertical axis is damage level. It was found that the strain value of instrument stepwise decreased as severity of injury is increased. From this result, we considered that strain value of our instrument could evaluate spinal instability very easy. Therefore, it was thought that our measuring instrument was a tool suitable for clinical.

4. Result and discussion of clinical application

Clinical application examined the relation between intervertebral range of motion (preoperatiove) and strain of our instrument (intraoperative) in the lumbarvertebrae. Result of clinical application is shown in Fig. 4, horizontal axis is intervertebral ROM (ROM : Range of Motion) and vertical axis is strain of our instrument. With regard to the relation between ROM and strain, correlation coefficient was –0.75 ($p<0.001$). Therefore we think that significant negative correlation was observed between them. Next, with regard to five dots enclosed by

dotted line, the angle of ROM showed normal value. However, strain value of our instrument showed low (instability) value. Actually, there were instability in these intervertebrae at the time of intraoperative diagnosis by surgeon. Therefore it was suggested that ROM could not be measured accurately by the pain in patients at the time of preoperative radiography. Furthermore, measuring time of our instrument was about 5 seconds for one session. From this result, it's just conceivable that procedure of our instrument is extremely easy. Therefore, it was thought that our instrument was suitable for the clinical application.

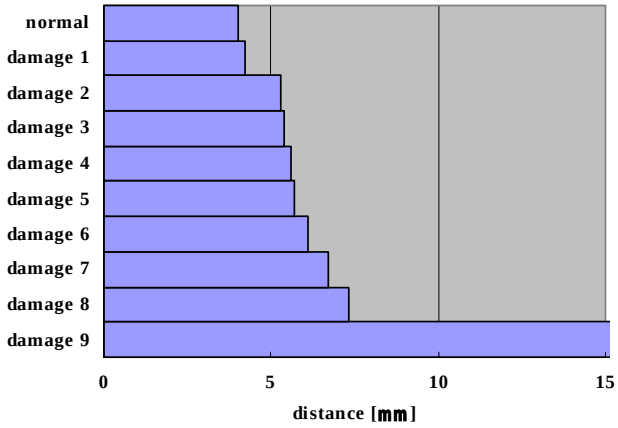

Fig.1 Relationship between damage and distance

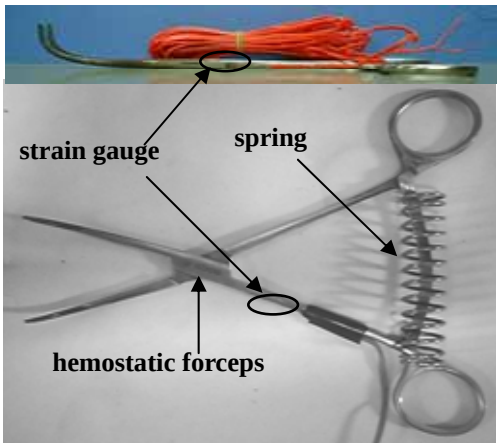

Fig. 2 Measuring instrument

5. Summary

Development of the measuring instrument that can evaluate lumbar spinal instability during an operation which aims at practicality was tackled in this research. Consequently, the following things were understood.

- Lumbar spinal instability was simply evaluated by relationship between force and displacement on only one direction between spinous processes.
- The strain value of our measuring instrument was stepwise decreased as severity of injury is increased.
- Significant negative correlation was observed between intervertebral ROM and strain value of our instrument.
- Our instrument could be an aid for selection of treatment strategy and surgical technique, because it had extremely easy method and simple structure.

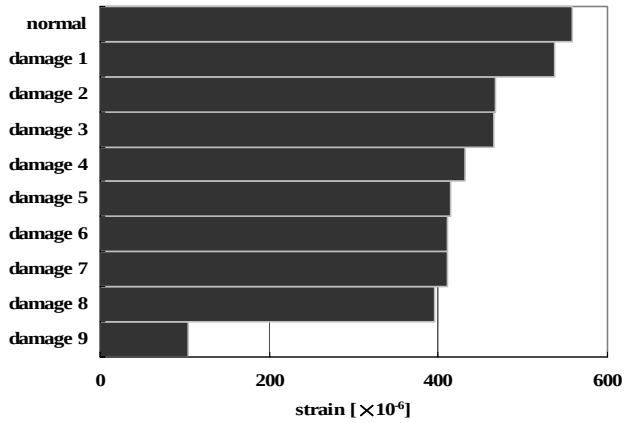

Fig. 3 Relationship between damage and strain

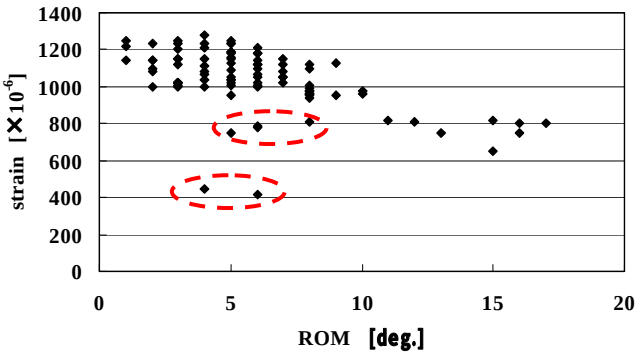

Fig. 4 Relationship between strain and intervertebral ROM

Author's publications

[1] Takaya KATOH, Yuichi KASAI, Tadashi INABA, Atsumasa UCHIDA and Masataka TOKUDA, Development of intraoperative measurement device for intervertebral instability [in Japanese], Journal of the Japanese Society for Clinical Biomechanics, Vol.24, pp.99-103, 2003

[2] Takaya KATOH, Yuichi KASAI, Tadashi INABA, Atsumasa UCHIDA and Masataka TOKUDA, Influence of rod diameter given to the internal pressure on the intervertebral disc and the screw in the thoracolumbar anterior spinal instrumentation [in Japanese], Journal of the Japanese Society for Clinical Biomechanics, Vol.25, pp.129-132, 2004

[3] Takaya KATOH, Yuichi KASAI, Tadashi INABA and Masataka TOKUDA, Development of Simple Measuring Instrument for Lumbar Spinal Instability [in Japanese], Trans. of the JSME, Series A, Vol.71, No.703, pp.494-499, 2005.

Gene Engineering Studies on Host Range Expansion of Viruses

Kenichi Maegawa
(Materials Science, Division of Materials Science)

Keywords: Host Range Expansion, Baculovirus, AnPe, AcNPV

In the animal kingdom, the host range of viruses is generally determined by interactions between defense mechanisms of host and escape mechanisms of pathogen and thus restricted as defined as host specificity. Host range expansion is to overcome the restriction of host range, which naturally occurs with evolutions and mutations of viruses. Virus-infectious diseases expanded to human from other animals such as measles, influenza, and severe acute respiratory syndrome (SARS) are typical examples of the host range expansion. The efforts to understand the mechanisms governing host range determination and factors involved in it would provide important implications to developments of vaccines and antiviral agents. Control of the host range could be achieved by artificial recombination of genes involved in the host range, and effective techniques for gene transfer into mammalian cells might also be developed. In other words, host range expansion is a natural and artificial technique for breakdown of a barrier of host specificity and available for a counter-plan for virus-infectious diseases.

Host range expansion is also available for a large scale-production of proteins in gene expression systems, for instance, in baculovirus expression vector (BEV) systems. The BEV system using the combination of AnpeNPV with AnPe cells and *A. pernyi* diapausing pupae has several advantageous characteristics for expression of large amounts of heterologous genes. In addition, the structure of some *N*-glycans added to the recombinant glycoprotein in AnPe cells is a bianntenary complex type, which is not detected in Sf9 insect cells. On the other hands, although AcNPV is most extensively used as a BEV, it does not infect successfully to AnPe cells and *A. peryni* diapausing pupae. Thus, AcNPV vectors cannot be utilized in AnPe cells and diapausing pupae of giant wild silkmoths as options for the recombinant protein production unless productive infection of AcNPV in *A. pernyi* cells is achieved by gene engineering.

Host range determinants of baculoviruses are poorly understood. Among them, *p143* gene product, putative DNA helicase, has been identified by comparing host ranges determinant between AcNPV and BmNPV, and replacement of the AcNPV *p143* gene with the homologous region from BmNPV *p143* gene enables AcNPV to replicate in nonpermissive BmN cells. Recently, a comparative genome map of AnpeNPV aligned with the fully sequenced OpMNPV genome was constructed, and cathepsin and chitinase genes of AnpeNPV has been identified in the genome by using this map. This genome map can also be used for identifying the *p143* gene which encodes putative DNA helicase. In the present thesis, thus, to understand the mechanisms governing host range between baculoviruses, the effect of the AnpeNPV *p143* gene on the host range expansion and the medium-dependent susceptibility to AcNPV infection in AnPe cells were investigated based on gene engineering.

In chapter 1, to investigate an accuracy of the genome map of AnpeNPV and to improve the BEV system using the combination of AnpeNPV with AnPe cell line and *A. pernyi* diapausing pupae, the *p10* gene, which is a very late gene with a strong promoter suitable for heterologous gene expression, was identified, and two transfer vector plasmids to generate recombinant AnpeNPV expressing heterologous genes were constructed. The *p10*

gene was found to exist within *Pst*I I fragment based on the comparative genome map between AnpeNPV and OpMNPV, and then, the 1873 bp nucleotide sequence within *Pst*I I fragment was determined, indicating that the AnpeNPV *p10* gene consist of the promoter sequence (55 bp) and coding sequence (264 bp) encoding 87 amino acids. The predicted amino acids sequence of the AnpeNPV *p10* gene product showed the highest identity (93%) to that of *Choristoneura fumiferana* NPV (CfNPV). The two transfer vector plasmids, pApp10 and pApCH3, were constructed, in which pApp10 was *p10* locus-based transfer vector plasmid containing *p10* gene promoter, and pApCH3 was a dual expression vector containing a copy of *p10* gene promoter inserted in the downstream of the polyhedrin promoter at tandem but opposite orientation. Results are attributable to development of recombinant AnpeNPV for mass production of foreign proteins and also demonstrated an accuracy of the genome map of AnpeNPV, suggesting that based on this genome map, certain genes involved in host range determination such as *p143* gene could be identified.

In chapter 2, to develop the host range expanded virus, the *p143* gene, one of the host range determinants, was identified from AnpeNPV genome based on the comparative genome map, and the effect on the host range expansion of the recombinant AcNPV, in which intact *p143* gene of AnpeNPV was introduced, was evaluated. The *p143* gene of AnpeNPV was sequenced and found to consist of coding sequence (3639 bp) encoding 1212 amino acids. Homology search for predicted amino acid sequence of the AnpeNPV *p143* gene was performed and found to have high identity (58%) and similarity (76%) to that of AcNPV. The recombinant AcNPV carrying the intact *p143* gene of AnpeNPV expressed the gene in AnPe cells, but BV production and heterologous gene expression were not enhanced, suggesting that the introduction of AnpeNPV *p143* gene into AcNPV genome did not affect the host range of AcNPV in semipermissive AnPe cells.

In chapter 3, medium-dependent AcNPV susceptibility in AnPe cells was investigated. First, BV titers and accumulations of polyhedrin in AcNPV-infected AnPe cells were analyzed by real-time PCR and SDS-PAGE, using AnPe cells adapted from both Sf-900II medium and TC-100 medium containing 10% FBS to their mixture of equal volumes and from Sf-900II alone to Sf-900II containing 10% FBS, and were found to be altered depending on culture media, indicating that host range of AcNPV could be controlled by culture media. Second, cellular transcripts expressed differentially by culture media have been examined using the differential display and the real-time RT-PCR methods, and five transcripts exhibited obvious differences in expression level (more than two-fold) between the two media have been identified. Homology search analysis has revealed that three transcripts of the five, which are abundantly expressed in the Sf-900II-maintained cells, show homologies to sequences of the genes involved in insect immunity. Third, comparative analyses of BV titers, polyhedrin production and expression level of 5 medium-responsive genes in the AcNPV-infected AnPe cells under different medium conditions has indicated that both AcNPV susceptibility and expression of medium-responsive genes are affected mainly by the balance of components contained in FBS and Sf-900II. It has been also suggested that gene products involved in insect immunity plays an important role for the host range determination.

Overall, the present study demonstrates that the improvement of a novel BEV system using combination of AnpeNPV with AnPe cell line was successful, and by supplementation of FBS to culture medium, the host range of AcNPV can be expanded, suggesting a possibility that the host range of baculoviruses can be controlled by medium components. This must contribute to improvements and developments of novel BEV system to enable mass production of various useful proteins.

Recently, innate immune systems were found to play an important role against virus infection as well as bacterial infection. Thus, the present study also suggests that activation of the innate immune system might suppress the diseases by emerging virus infection such as SARS, AIDS and Ebola hemorrhagic fever, and understanding the innate immune system could facilitate development of novel gene transfer vector into mammalian cells and insect cells.

Synthesis of Poly(methacrylate)s with Semipolar Structures on the Side Chains, and Their Solution and Film Properties

Tomoaki Hiwatashi †

Key Words: Charged polymer, Polyelectrolyte, Polyzwitterion, Anti-polyelectrolyte Behavior, Viscosity Behavior, Composite, Mechanical Property, Surface Property

1. Introduction

Currently ion-containing water-soluble resins can be broadly categorized as an anionic, cationic, nonionic or amphoteric resin. These polymers are utilized as basic materials for water remediation, reagents, thickeners, and formulation of pharmaceuticals, coating, and cosmetics. One of the required behaviors of the polymers is e.g. to that they do not lower their viscosity with the addition of electrolytes. Therefore, studies are focused on finding methods for synthesizing water-soluble polymers that will not lower viscosity with the addition of electrolytes. Recently, polyampholytes containing cationic and anionic functionality on different mer units and polyzwitterions having both charges on a single mer unit were synthesized and their solution properties have been investigated. Since common polyelectrolytes have ionizable functional groups that are either cationic or anionic and the charges are balanced by small gegenions or counterions, the polymer chain tends to extend due to the charge-charge repulsions, resulting from counterion mobility, in water at low polymer concentration. When common polyelectrolytes encounter small electrolytes such as inorganic salts, they tend to shrink by the "shield effect". In contrast, charge-balanced polyzwitterions having both positive and negative charges tend to expand due to reduced intramolecular attractions, when the polymer encounters small electrolytes (Scheme 1). This latter polyzwitterion behavior is termed the "anti-polyelectrolyte effect". The addition effect of small electrolytes on the solution viscosity behavior of polyzwitterion using sulfobetaine as a typical "anti-polyelectrolyte" with both positive and negative charges on a single mer unit has been aggressively studied.

Recently, zwitterions having a carboxybetaine group, an amine *N*-oxide group and a sulfoxide group are in the spotlight in the surfactant area, because they have proved to improve the performance of surfactant, emulsion or dispersion. In particular, it is reported that the behavior of a zwitterion surfactant (i.e. carboxybetaine surfactant) bearing both positive and negative groups (for example: ammonium, carboxyl group) on a single mer unit is similar to a nonionic surfactant with respect to micelle formation. It is also reported that the property of electrolytes having a semipolar bonding group like *N*-alkylaminoalkane imide or sulfoimide are similar to that of nonionic surfactant with respect to micelle formation and to other factors because positive and negative groups in the molecule are fixed by a covalent bond.

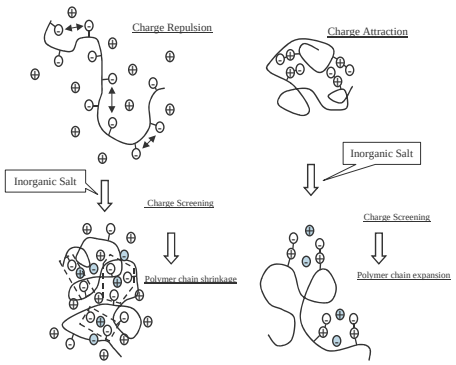

Scheme 1

† Coating Material Laboratory, Mitsubishi Chemical Corporation

In this work, a *N*,*N*-dimethyl-*N*-(2-methacryloyloxyethyl)amine *N*-oxide polymer (poly(DMANO)), which is classified as an amine *N*-oxide type semipolar resin, was prepared and its solution property as a polyzwitterion was investigated on the base of the viscosity behavior in aqueous solutions, pH dependence, and the change in viscosity behavior by the addition of inorganic salt. And, we prepared three series terpolymers composed of 1) *N*,*N*-dimethyl-*N*-(2-methacryloyloxehyl)amine *N*-oxide, methyl methacrylate (MMA) and IBMA (DMANO-series), as novel semi-polar resins belonging to amine oxide type, 2) *N*,*N*-dimethyl-*N*-(2-methacryloyloxy)ethylammonioacetate, MMA and IBMA (DMEAA-series), and 3) *N*-(ethyl)-*N*,*N*-dimethyl-*N*-(2-methacryloyloxyethyl) ammonium ethylsulfonate, MMA and IBMA (EDMES-series), and we investigated the surface properties and mechanical properties of their anti-polyelectrolyte films.

2. Experimental and results

2.1. Synthesis and Solution Properties of Poly(methacrylate)s with Semipolar Structure on the Side Chain

Three charged polymers, poly(DMANO), poly(EDMES) and poly(DMEAA), were prepared by the reaction of poly(DMMA) with hydrogen peroxide, chloroacetic acid and diethyl sulfate, respectively. The solution properties were investigated on the basis of viscosity behaviors. The solution viscosity behavior of the poly(EDMES) proved to be that of a common polyelectrolyte and the behaviors of the other two polymers to be those of anti-polyelectrolytes. It was found that the poly(DMANO) is a unique charged polymer that is different from the poly(DMEAA) with respect to the viscosity in aqueous solutions, because it behaves differently with a change in pH. i.e., it behaves like a cationic polyelectrolyte under acidic condition and like a polyzwitterions (anti-electrolyte) as a *N*-oxide polymer under neutral to alkaline conditions.

2.2. Terpolymer films having semipolar structure: Preparation, Wettability, and Mechanical Property

A terpolymer, obtained by the terpolymerization of 2-(*N*,*N*-dimethylamino)ethyl methacrylate (DMMA), methyl methacrylate(MMA)and isobutyl methacrylate(IBMA), was allowed to react with hydrogen peroxide, chloroacetic acid and diethyl sulfate to form corresponding modified terpolymers, 1) *N*,*N*-dimethyl-*N*-(2-methacryloyloxyethyl)amine *N*-oxide, MMA and IBMA (DMANO-series), 2) *N*,*N*-dimethyl-*N*-(2-methacryloyloxy)ethylammonioacetate, MMA and IBMA (DMEAA-series), and 3) *N*-(ethyl)-*N*,*N*-dimethyl-*N*- (2-methacryloyloxyethyl) ammonium ethyl sulfonate, MMA and IBMA (EDMES-series), respectively. Using ^{13}C-NMR analysis, terpolymer composition was confirmed to have the same composition for monomers (starting materials) reacted. Based on the observation of the surface free energies of the terpolymers, which were obtained from the data of water contact angle and methylene iodide on the films, it was found that the upper surface of the films for the DMANO- and DMEAA-series are more hydrophobic than that for the EDMES-series. The comparison of mechanical properties by measuring stress-strain test between two specimen clarified that DMANO-series was a unique polymer having larger elongation to break (smaller Young's modulus) than DMEAA-series due to the existence of hydrated water in DMANO-series.

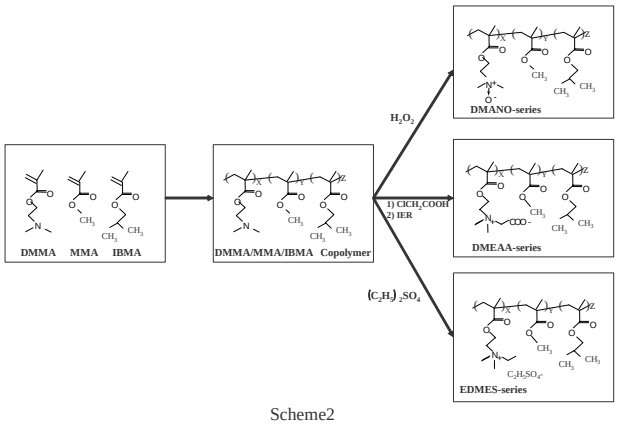

Scheme2

Auther's Publications

[1] Hiwatashi, T. ; Hayama, K.; Sawada, Y.; Itoh, T. J. Polym. Sci.: Part A: Polym. Chem. 2005, 43, 129.

[2] Hiwatashi, T. ; Hayama, K.; Sawada, Y.; Itoh, T. J. Applied Polym. Sci , in press.

Abstracts of Doctor's Thesis

Study on the Sol-gel preparation, properties and structure of titanophosphate glasses with high titanium dioxide contents

Anjiang Tang*

Keywords: Glasses; Sol-gel chemistry; Optical properties; Coordination number; 6-fold coordination

1. Introduction

Based on nonlinear optical effects of materials, e.g., changes in the refractive index and/or absorption coefficient caused by an intense optical beam (laser-beam), photonic or optical devices are designed to switch and process light signals without converting them to the electronic form. For applications such as the optical switching by using laser light, the third order nonlinear susceptibility $\chi^{(3)}$ is needed to be of the order of larger than 10^{-8}~10^{-9} esu. In addition, based on the semi-empirical rules which predict the $\chi^{(3)}$ as a function of the refractive index and/or the optical band gap, the titanium oxide (TiO_2) is a promising nonlinear optical material due to its large refractive index (>2.5). The glass is one of attractive and useful materials in the field of optical applications. Glasses containing a large amount of titania are expected to have high refractive index and considered to be promising nonlinear optical materials. However, the solubility of titania in silica is not high enough to attain the refractive index as high as 2.0. We know that only P_2O_5 can dissolve titania up to about 70 mol%. Unfortunately, up to now, the maximum TiO_2 content which allows glass formation by melt-quenching method is 74 mol%. This thesis presents the results of study on the sol-gel preparation, fundamental optical properties and structure of TiO_2-P_2O_5 glasses with higher TiO_2 content.

2. Research Methods

This method uses the metal alkoxide as raw material, alcohols as solvents, acids as the catalyst (seen fig.1). The sol-gel chemistry consists of hydrolysis and condensation reactions to form gel, then heat-treating the gel to prepare the glass, or by dip-coating to prepare the glass film.

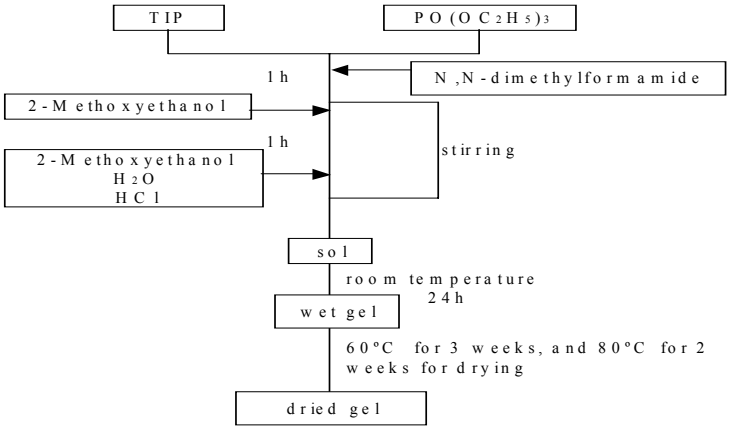

Fig. 1. Folw chart for preparation of the TiO_2-P_2O_5 bulk gels.

3. Results and Discussion

These bulk glasses are highly transparent and colorless as shown in fig.2. Densities, refractive

indices and other of these bulk glasses are listed in Table 1, which was higher than that of the corresponding melt-derived glass. The coordination number of Ti^{4+} ions was evaluated to be almost 6 in the sol-gel glasses, while 4-5 in the melt-glass, from X-ray atomic distribution function analysis and IR, Raman spectroscopy.

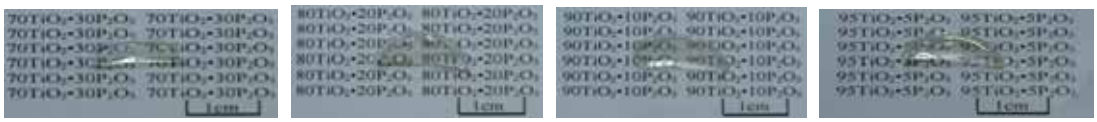

Fig. 2. Photographs of the sol-gel bulk glasses.

Table 1. Compositions (mol%) and some properties of $xTiO_2 \cdot (100\text{-}x)P_2O_5$ bulk glasses prepared by the sol-gel method.

No.	Batched		Analysed		T_g	T_p	ρ (measured)	ρ (calculated)	$n_{632.8}$
	TiO_2	P_2O_5	TiO_2	P_2O_5					
	mol%		mol%		°C	°C	$g \cdot cm^{-3}$	$g \cdot cm^{-3}$	
1	70	30	73	28	622	779	3.26	3.26	2.099
2	80	20	78	19	631	804	3.39	3.42	2.121
3	90	10	86	13	650	828	3.20	3.63	2.204
4	95	5	93	10	670	868	3.13	3.75	2.264

4. Conclusions

(1) Ti^{3+}-free, transparent and colorless monolithic bulk-shaped TiO_2-P_2O_5 glasses containing very large amount of TiO_2 (up to 95 mol%) were successfully prepared by sol-gel method.

(2) Glasses of TiO_2 content of larger than 80 mol% possessed very high refractive index as 2.1-2.3.

(3) It was found that 6-fold coordinated Ti^{4+} ions were abundant in the sol-gel-derived glasses. Larger density and higher refractive index of the sol-gel-derived glasses were ascribed to more abundance of 6-fold coordinated Ti^{4+} ions.

(4) Glass coating films of $xTiO_2 \cdot (100\text{-}x)P_2O_5$ (x = 70 and 80 mol%) compositions of high refractive index were also prepared by the sol-gel method.

Author' publications

[1] A. Tang, T. Hashimoto, H. Nasu and K. Kamiya, "Sol-gel preparation and properties of TiO_2-P_2O_5 bulk glasses", Mat. Res. Bull., **40** (1) (2005) 55-56.

[2] A. Tang, T. Hashimoto, T. Nishida, H. Nasu and K. Kamiya, "Structure study of binary titanophosphate glasses prepared by sol-gel and melting methods", J. Ceram. Soc. Japan, **112** (9) (2004) 467-472.

[3] A. Tang, T. Hashimoto, H. Nasu and K. Kamiya, "Structure study of TiO_2-P_2O_5 glasses prepared by sol-gel method", Proceedings of 20th International Congress on Glass, Kyoto, 2004, CDROM (O-10-021), pp.1-6.

[4] A. Tang, "Sol-gel preparation and properties of TiO_2-P_2O_5 glass films", to be published.

Life Cycle Analysis and Assessment of Vending Machines, and their Eco-Improvement

Yukio Kimura
(Division of Systems Engineering)

Keywords: Vending Machine, LCA, LCA-*NETS*, LCC, ECP, reuse

Objective:

Vending machines are required to support solutions to various environmental-related problems and to comply with applicable legal statutes and regulations. Meanwhile, industrial and engineering considerations have led to requests for the establishment of "ECP design tools" that will enable innovative environmental technology. Life cycle assessment (LCA) is an engineering method for quantitatively measuring and assessing the impact that an industrial product imposes on the global environment during that product's lifecycle. LCA is a powerful method for finding solutions to the abovementioned problems. This paper describes the environmental technology processes and eco-improvements (ecological and economical improvements) achieved through the successful application of LCA to vending machines.

Contents:

Chapter 1: The history of LCA and the process for establishing relevant ISO and JIS standards are described. Activities in Japan by the LCA Japan Forum and throughout the world by the Global Alliance for Life Cycle Assessment Centers (GALAC) toward practical application of LCA are discussed. Additionally, trends in life cycle costing (LCC)—a cost oriented assessment—and in CO2 emissions trading according to the Kyoto Protocol are discussed.

Additionally, environmental technology-related problems in order to achieve greater use of ECPs are identified through the situation that vending machine use becomes widespread, and the importance of LCA-based designs to resolve those problems by reducing the impact on the environment and the value and significance of our research are described.

Chapter 2: Because the causal relationships concerning environmental impacts are often ambiguous, assessments from only one viewpoint are meaningless. Particularly in the case of industrial products that are distributed widely throughout the world, it is generally necessary to introduce an integrated methodology that employs universal and objective measures. The integrated LCA scheme "LCA-*NETS*," developed independently at the authors' research laboratory, and its theory (L-R Tolerant Balance Theory) are described.

Chapter 3: A vending machine model that typically sells 20 types of canned beverages was selected, dismantled, and the mass of each category of materials was measured and then input as an ID into the analysis software *MieLCA* in order to analyze and assess that vending machine. The results revealed a large environmental impact on global warming and fossil fuel depletion due to CO2 emission associated with the consumption of power at the operating stage over the course of a 5-year service life. This suggests that energy savings measures are important for vending machines. Moreover, the materials procurement stage also exhibited a large impact on the environment arising from the depletion of natural resources, and this demonstrated the importance of reducing the quantity of, and reusing and recycling of the materials used. In reviewing the history of development and model changes from 1993 through 2000, it can be seen that a dramatic 41% reduction in total environmental impact had been achieved by 2000. This result reflects the successful adoption of LCA-based eco-improvement measures to conserve energy at the operating state and to reduce the quantities of materials used at the procurement stage.

Chapter 4: After examining the potential for realizing eco-improvement, we returned to the beneficial concept of reusable parts. Specifically, the reduction in environmental impact achieved through reuse of the main 4 blocks (that previously had been replaced every 5 years) was analyzed and assessed. The results revealed that, if used for 10 years, the total environmental impact could

be reduced by 24%. Particularly, the impact due to the problems of natural resource depletion and waste materials could be reduced by 25% and 31%, respectively. However, in order to achieve actual reuse that is significant in terms of both LCA and LCC, the product design stage must be considered, and the ease of installation/removal and the quality control (parts manifest) of the reusable parts are important factors. Additionally, as a part of the lease management of vending machines, the necessity for establishing an ECP control system that covers the entire life cycle until final disposal is also supported by the findings of the LCA-based assessment.

Chapter 5: This chapter presents the conclusions of the paper. A summary of each of the abovementioned chapters is provided, and in consideration of the environmental elemental technologies that were successful in reducing the environmental impact of vending machines, technical measures for furthering the use of ECP industrial products are proposed.

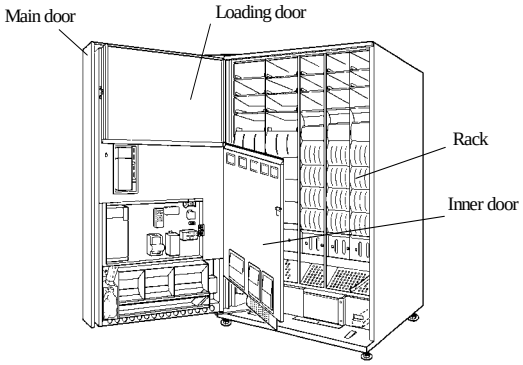

Structure of a typical can vending machine.

Materials composing a vending machine.

Material	Weight [kg / unit] '93 machine	'98 machine	'99 machine	'00 machine
Iron	279.0	223.8	198.6	191.3
Copper	8.9	7.6	7.3	7.3
Aluminum	2.7	2.3	1.3	1.3
Zinc	0.6	0.7	0.8	0.8
Plastics	23.2	18.8	22.8	22.6
Rubber	0.4	0.2	0.2	0.2
Other (paper, etc.)	4.7	2.2	3.0	3.1
Oil for refrigerating machine	0.2	0.2	0.2	0.2
CFC-11	0.7	-	-	-
CFC-12	0.3	-	-	-
HCFC-22	-	0.3	0.2	-
HFC-407C (for refrigerant)	-	-	-	0.2
HCFC-141b (for insulation)	-	0.9	0.9	0.9
Total	320.7	257.0	235.3	227.9

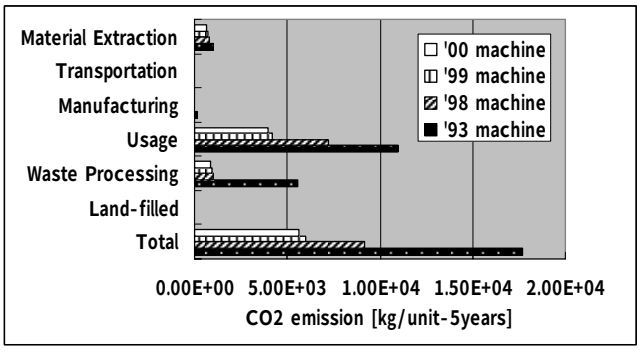

CO_2 emission from machines (5 years).

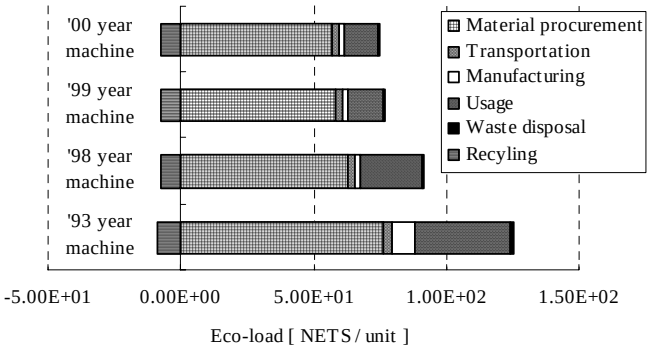

Integrated environmental impacts by can vending machines at each life cycle stage.

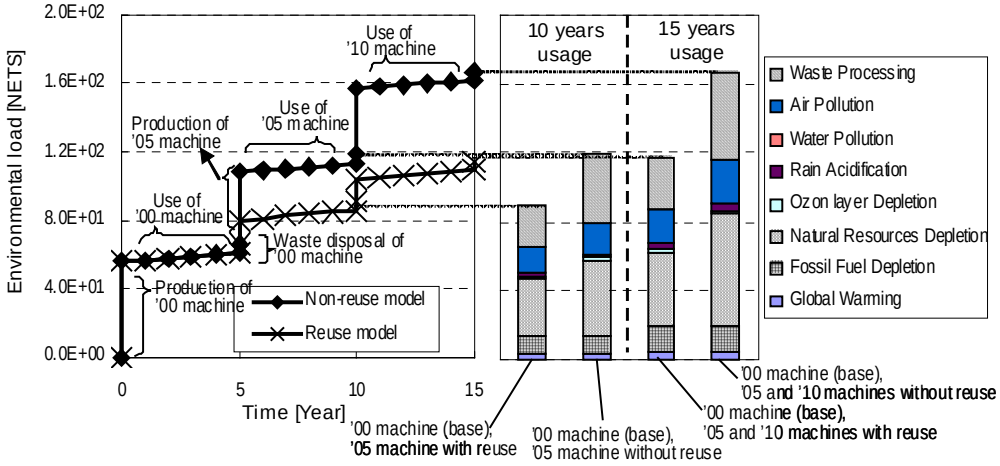

Remarkable reduction of integrated environmental load with the aid of 4 blocks reuse.

Study on Improvement Mechanism of Quality of Vacuum Processed Concrete Based on Consolidation Theory

Hiroki Hattori*
(Department of Architecture, Division of Systems Engineering)

Keywords: Vacuum processing method, Consolidation theory, Pore water pressure distribution, Ingredient analysis, Density distribution, Strength distribution

1. Contents of thesis

This thesis is composed of Chapters 1 to 7. Table 1 shows contents of this thesis.

Table 1 Contents of thesis

2. Abstract

The strength and hardness of concrete slab surface is considered significantly affected by bleeding of concrete. It has been reported that dewatering by vacuum processing is quite effective to make concrete high density and high strength. The method, however, has not been successfully used for the concrete works in the field of building construction, compared with that of civil engineering works in Japan.

In the earlier report, the authors have already pointed out that there is a strong relationship between the strength distribution and density distribution in the vacuum processed concrete, both gradually decreasing from the top surface to about 15 cm depth of concrete. Main purpose of the present study is to discuss the mechanism of the occurrence of such distribution of strength and density, based on consolidation theory. In the experiment, pore water pressure distribution in concrete has been measured

* Tokyu Construction Co., LTD.

using the original measuring system. As a result, it has been confirmed that the consolidation theory is quite effective to explain the internal properties of vacuum processed concrete as well as those of press-dewatered concrete. Also, this thesis reports the results of the investigation on the distribution of ingredients in both mortar and concrete. Further, a prediction method for the strength improvement of concrete by vacuum processing is discussed. Figure 1 shows prediction flow of the density distribution and strength distribution.

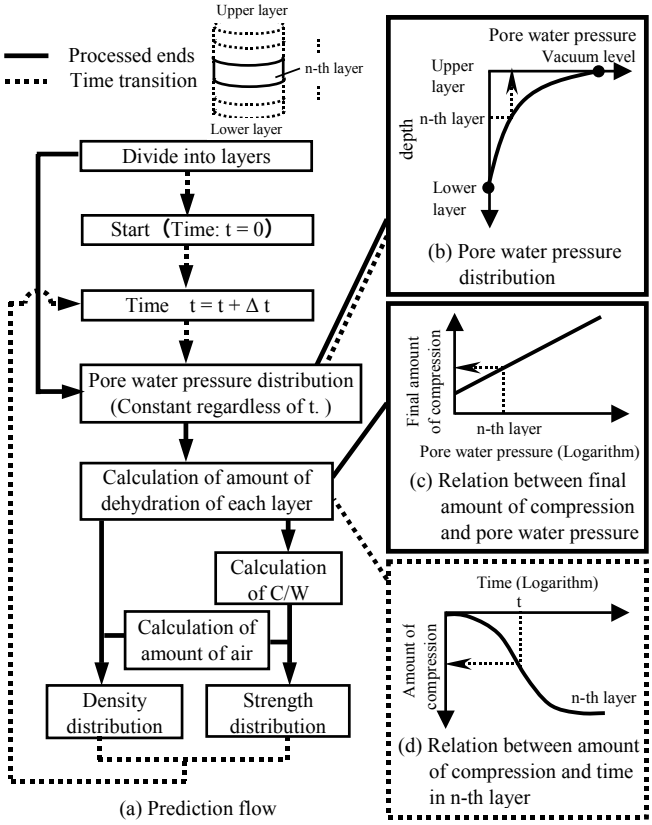

Figure 1 Prediction flow of density distribution and strength distribution

3. Papers list

(1) Papers in reviewed journals

1) H. Hattori, S. Hatanaka, N. Mishima and H. Wato: Fundamental Study on Compaction Mechanism of Mortar Based on the Consolidation Theory, Proceedings of JCI, Vol.25, No.1, pp.881-886, 2003.7.
2) H. Hattori, S. Hatanaka, E. Sakamoto and N. Mishima: Fundamental Study on Compaction Mechanism Based on the Consolidation Theory, Proceedings of JCI, Vol.26, No.1, pp.1227-1232, 2004.7.
3) H. Hattori, E. Sakamoto, N. Mishima and S. Hatanaka: Experimental Study on Compaction Mechanism of Vacuum Processing Method Based on the Consolidation Theory, Proceeding of JCI Symposium on Quality Improvement of Concrete by Drainage and Dewatering, pp.299-306, 2004.9.
4) H. Hattori, S. Hatanaka, N. Mishima and E. Sakamoto: Fundamental Study on Compaction Mechanism of Vacuum Processing Method Based on the Consolidation Theory, Journal of Structural and Construction Engineering, AIJ, No.585, pp.7-13, 2004.11.
5) S. Hatanaka, H. Hattori, E. Sakamoto and N. Mishima: Study on Mechanism of Strength Distribution in Vacuum Processed Concrete Based on the Consolidation Theory, Journal of Structural and Construction Engineering, AIJ, (in press)

(2) Oral announcement papers

1) H. Hattori, N. Mishima, H. Wato and S. Hatanaka: Study on Compaction Mechanism of Vacuum Processing Method Based on the Consolidation Theory, Research reports of Tokai branch, AIJ, No.40, pp.17-20, 2002.2.
2) H. Hattori, N. Mishima, H. Wato and S. Hatanaka: Experimental Study on Compaction Mechanism of Mortar Based on the Consolidation Theory, Summaries of Technical Papers of Annual Meeting, AIJ, A-1, pp.471-472, 2002.8.
3) H. Hattori, N. Mishima, H. Wato and S. Hatanaka: Prediction of Density Distribution in Mortar Dewatered by Pressure Based on the Consolidation Theory, Research reports of Tokai branch, AIJ, No.41, pp.25-28, 2003.2.
4) H. Hattori, E. Sakamoto, N. Mishima and S. Hatanaka: Experimental Study on Compaction Mechanism Based on the Consolidation Theory, Research reports of Tokai branch, AIJ, No.42, pp.129-132, 2004.2.
5) H. Hattori, N. Mishima, H. Wato and S. Hatanaka: Experimental Study on Pore Water Pressure Distribution in Mortar and Concrete during Vacuum Processing (Part1. Outline of Experiment), Summaries of Technical Papers of Annual Meeting, AIJ, A-1, pp.245-246, 2004.8.
6) H. Hattori, N. Mishima, H. Wato and S. Hatanaka: Experimental Study on Pore Water Pressure Distribution in Mortar and Concrete during Vacuum Processing (Part2. Experimental Results and Discussion), Summaries of Technical Papers of Annual Meeting, AIJ, A-1, pp.247-248, 2004.8.
7) H. Hattori, E. Sakamoto, N. Mishima and S. Hatanaka: Fundamental Study on Mechanism of Strength Distribution in Vacuum Processed Concrete (Part 1. Purpose and Outline of Experiment), Research reports of Tokai branch, AIJ, No.43, pp.85-88, 2005.2.
8) E. Sakamoto, H. Hattori, N. Mishima and S. Hatanaka: Fundamental Study on Mechanism of Strength Distribution in Vacuum Processed Concrete (Part 2. Experimental Results and Discussion), Research reports of Tokai branch, AIJ, No.43, pp.89-92, 2005.2.

Study of e-Learning System to Encourage Spontaneous Learning from Mistakes

TABATA Shinobu
(Educational Technology, Division of Systems Engineering)

Keywords: e-Learning, review of incorrect answer, confidence in answer

1.The purpose

The purpose of practice is to provide feedback to learners in order to improve their comprehension. To improve the comprehension, the learners should review the questions that they could not make correct answers according to teachers' advice. However, only a few learners conduct reviews on their own initiative. I propose a practice system of e-Learning in order to promote learners' incorrect answers.

2.Idea

Learners want to find how to solve the questions and they revise their answers, if they have confidence in their answers but it is incorrect. Meanwhile, if they do not have confidence and their answers are incorrect, they tend to accept it as a matter of course and they do not review the answers. In the traditional practice systems, learners are forced to answer to questions whether they have confidence or not, and they sometimes answer without confidence.

I propose a practice system of e-Learning based on the idea that learners should not be forced to make any answers without confidence. Using the system, it is expected that learners revise their incorrect answers.

3. Proposed system

The practice system of e-Learning has four components –calculation question's component (Fig.1), multiple-choice question's component (Fig.2), discription question's component (Fig.3), problem-posing component (Fig.4,5). Calcuation question's component displays part of answer stepwise according to students requests. Multiple-choice question's component displays explanations of each alternative if students cannot answer with confidence. Discription question's component displays keywords and explanations. Prpblem-posing component added the following two phases to the traditional one. (1) Students describe the explanation of the

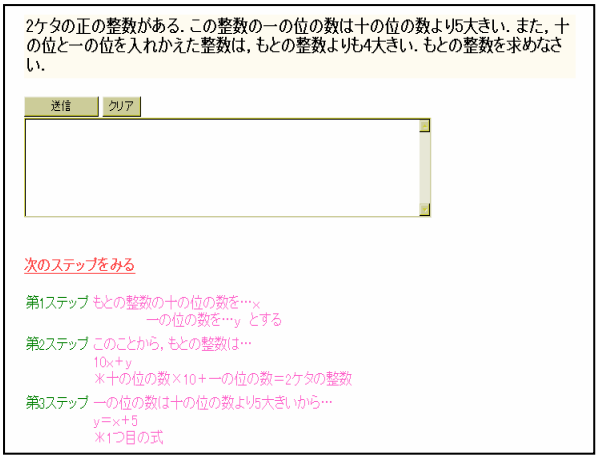

Fig.1 Calculation question's component

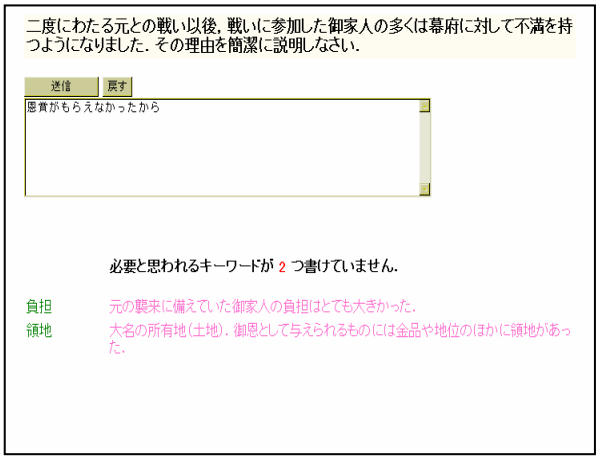

Fig.2 Multiple-choice question's component

solving methods when they create problems. (2) Students check over the created problems and explanations to each other. These two phases make the students confirm the solving methods of the problems and improve their understanding.

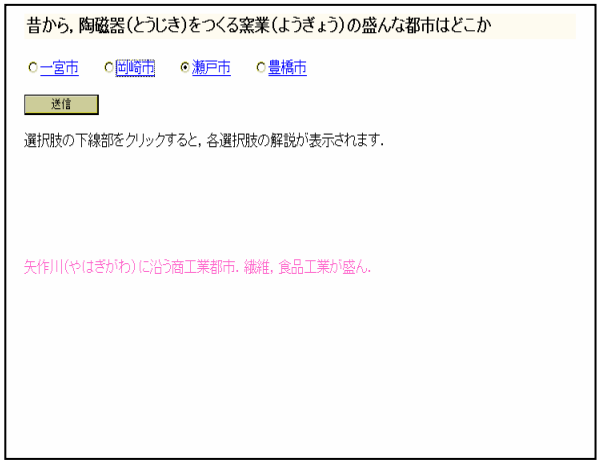

Fig.3 Description question's component

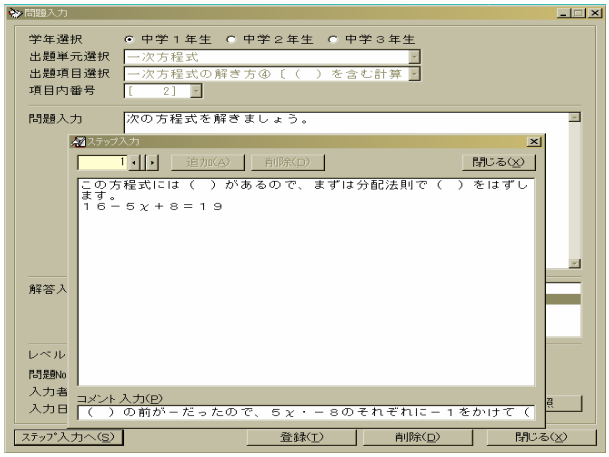

Fig.4 Problem-posing component (Create explanation)

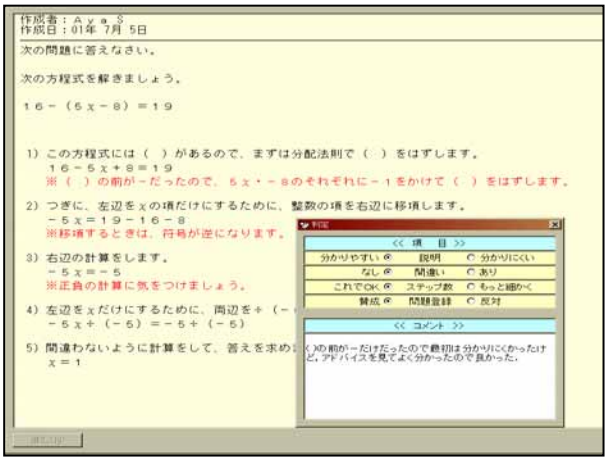

Fig.5 Problem-posing component (Check over the explanations to each other)

4.Experimental Use and Results

I experimentally used the system in math classes, history classes and science calsses of junior high school and cramming school. The results of the experiment show the effectiveness of the system.

Statistical Approaches to Detecting Article Errors in the Writing of Japanese Learners of English

Ryo Nagata

(Artificial Intelligence, Division of Systems Engineering)

Keywords: Article, Learners of English, Corpus, Mass Count Distinction, Error detection

One of the big problems Japanese learners of English have in English writing is the usage of the articles. It is difficult for them to use the articles properly, perhaps because the Japanese language does not have an article system similar to that of English. Consequently they often make article errors in English writing (e.g., an information). Correlated with this is the usage of mass and count nouns. The Japanese language also has no or little conception of mass and count nouns. Because of the reason, mass nouns are often used improperly as count nouns in the writing of Japanese learners of English and vice versa (e.g., informations).

In view of this fact, this thesis describes several novel approaches to detecting errors concerning the articles and the mass/count usage. All approaches are based on statistics derived from a set of texts called corpus. They also exploit linguistic knowledge.

Before taking any approach to detecting article errors, it is important to know what type of errors appears in what proportion in the writing of Japanese learners of English. Chapter 2 describes taxonomy of the errors. For example, this chapter shows that a majority of the errors are missing articles in it, which suggests that algorithms for detecting the errors should be designed focusing on missing articles.

Taking the taxonomy into consideration, Chapter 3 introduces a simple statistical model for detecting the errors. The model exploits uneven distribution of the usages of the articles and singular/plural. For example, the noun ``information'' is rarely modified by the indefinite article nor is in plural form, which suggests ``an information'' and ``informations'' might be errors on the assumption that they do not know the rare usage and therefore mistakenly use it. Statistics derived from a corpus indicate which case is rare and how rare it is. For instance, ``information'' appears 701 times in the EDR corpus, and of those 13 (2%) and 0 (0%) are ``an information'' and ``informations'', respectively. This idea is formalized by conditional probabilities. Conditional probabilities that nouns are modified by the articles and are in singular/plural form are estimated based on statistics derived from a corpus. The conditional probabilities are used for generating rules for detecting the errors. Experiments show that performance of the model on essays written by Japanese learners of English is fairly well: Recall = 0.58, Precision = 0.76. It also turns out that the simple statistical model works well on some nouns and not on others. Possible reasons are discussed in the end.

Chapter 4 describes a more sophisticated model. In this model, statistics are combined with syntactic information. Linguists have shown that syntax has influence on the usage of the articles. For example, prepositional phrases have influence on the usage of the articles that modifies nouns in them (e.g., ``on the contrary''). So do verbs (e.g., ``take care''). In order to combine statistics with syntactic information, conditional probabilities are estimated looking at the three head words — the VP (Verb Phrase) head, the preposition, and the NP (Noun Phrase head) — instead of looking at just the NP head, which is adopted in the simple statistical model. Unfortunately, it requires a very large corpus to estimate conditional probabilities simply looking at the three head words. To abate the problem, this chapter also describes a method for estimating the conditional probabilities with a small corpus. Experiments show that the performance of the sophisticated model is Recall = 0.64 and Precision = 0.77, an improvement of 0.06 in Recall and 0.01 in Precision over the simple statistical model.

Chapter 5 describes a method for distinguishing mass and count nouns in context as an alternative approach. Many types of the errors can be easily detected given whether a noun in context is mass or count. For example, given that the ``chicken'' in ``I have chicken.'' is count, an error can be detected because a singular noun without any article is an error. Unlike the previous two, this approach works on nouns whose distribution of the usages of the articles and singular/plural is not uneven. In this approach, mass and count nouns are distinguished via contextual information. Here, contextual information refers to words surrounding the target noun in question. The surrounding words are good indicators of the target noun being mass or count. For example, the ``ate'' in ``She ate chicken.'' is a good indicator of ``chicken'' being mass because ``chicken'' in the sense of food is a mass noun. To exploit contextual information, words surrounding the target noun are corrected from a corpus using NLP (Natural Language Processing) tools and weighted based on their frequencies in the corpus. The weighted words are used for distinguishing mass and count nouns in novel context. Experiments show that the method correctly distinguishes mass and count nouns 83.9% of the time and that it is applicable to detecting the errors.

Chapter 6 presents closing discussions. As shown in the previous chapters, statistical approaches are effective to detecting the errors. Although the models are rather simple, they work as well as rules made manually or even better. In addition to its effectiveness, practicality is one of the distinctive features of the approaches. Statistics can be derived from a corpus using NLP tools and rules are automatically generated from the statistics. In other words, once a corpus is given and algorithms presented in this thesis are implemented, it takes no human intervention to generate rules and detect the errors. This is a big advantage of the approaches considering that it is costly and time-consuming to make rules manually. Other distinctive features are also described in this chapter.

3-D FEM Progressive Failure Analysis on Compressive Concrete Members with Strength Variation Due to Bleeding

Yukio YOSHIDA*
(Division of System Engineering)

Keywords: Confined Concrete, Bleeding, Strength Variation, 3-D FEM analysis, DIANA

1. Contents of thesis

This thesis is composed of Chapters 1 to 6. **Table 1** shows contents of the thesis.

Table 1 Contents of thesis

2. Abstract of papers

2.1 Compressive failure of circular confined concrete considering effect of interface element (Ref. 1), 3))

Two series of FEM analyses have been carried out. Firstly, the optimum values of internal friction angle ϕ and dilatancy angle ψ, used in the Drucker-Prager type of plasticity model with the strain softening effect, have been discussed for a single concrete element subjected to uniformly distributed lateral pressure. As a result, following values have been obtained, internal friction angle ϕ: 53 degrees, dilatancy angle ψ: e.g. 40 degrees for uniform lateral pressure of 1 MPa, and 30 degrees for 2 MPa. Secondly, simulation analyses have been carried out for the compressive behavior of circular concrete specimens confined by steel tubes or reinforcing bars, introducing interface element. As a result, it has been pointed out that the distribution of equivalent confining pressure σ_c along the longitudinal direction of a specimen and the progress of the degree of damage β in horizontal sections differ by element types applied to the confining steel and interface elements.

2.2 Compressive failure of circular confined concrete with Drucker-Prager model (Ref. 2), 5))

Main purpose of this study is to discuss the effect of parameters (e.g. internal friction angle ϕ and dilatancy

* Ai TECNICA Co.,Ltd.

angle ψ) of the constitutive law of Drucker–Prager type on the result of simulation analysis of confined concrete under compression. Two series of 3-D FEM analyses have been carried out. Firstly, the optimum values of the internal friction angle φ and dilatancy angle ψ, used in the Drucker-Prager type plasticity model with the strain softening effect, have been discussed for a set of compressive strength data of concrete specimens with different shapes. As a result, reasonable value as the internal friction angle φ has been found to be approximately 30 degrees for a condition of rather high equivalent lateral pressure σ_c. Secondly, simulation analyses have been carried out for the compressive behavior of circular concrete specimens confined by steel tubes or reinforcing bars, introducing interface element and different values of the internal friction angle φ. As a result, it has been pointed out that the distribution of equivalent confining pressure σ_c along the longitudinal direction of a specimen (see **Figure 1**) and the progress of the degree of damage β in horizontal sections differ to a large extent by the value of internal friction angle φ applied.

2.3 Compressive failure of circular concrete with strength variation due to bleeding (Ref. 4))

Purpose of this study is to discuss the compressive failure state and the effectiveness of internal friction angle used in the Drucker-Prager model, based on the uniaxial compression 3-D FEM analysis of plain concrete with the strength variation due to bleeding. As a result of analyses which introduced the different values of internal friction angle φ (30 and 53 degrees), it has been pointed out that 1) the failure zone L_p along the longitudinal direction of specimen shows tendency of proportional reduction with the increase in the size of a specimen, and 2) the distribution of equivalent strain inside a specimen obtained from the analysis with internal friction angle φ= 53 degrees can represent the ordinary failure pattern (see **Figure 2**).

3. Papers list

1) Y. YOSHIDA, E. MIZUNO and S. HATANAKA : FEM Analysis on Compressive Failure of Circular Confined Concrete Considering Effect of Interface Element, Journal of Structural and Construction Engineering, AIJ, No.563, pp.169-176, 2003.1 (in Japanese)

2) Y. YOSHIDA, S. HATANAKA and E. MIZUNO : Compressive Failure 3-D FEM Analysis of Cylindrical Confined Concrete with the Drucker-Prager Model, Journal of Structural and Construction Engineering, AIJ, No.587, pp.155-162, 2005.1 (in Japanese)

3) Y. YOSHIDA, E. MIZUNO and S. HATANAKA : FEM Analysis on Stress and Damage States inside Confined Concrete Cylinders, Proceedings of JCI, Vol.24, No.2, pp.97-102, 2002.6 (in Japanese)

4) Y. YOSHIDA, S. HATANAKA and E. MIZUNO: Size Effect FEM Analysis of Plain Concrete Cylinders with Bleeding Layers, Proceedings of JCI, Vol.25, No.2, pp.55-60, 2003.7 (in Japanese)

5) Y. YOSHIDA, S. HATANAKA and E. MIZUNO: Uniaxial Compression 3-D FEM Analysis of Cylindrical Concrete Specimens with Different Shape Ratios, Proceedings of JCI, Vol.26, No.2, pp.19-24, 2004.7 (in Japanese)

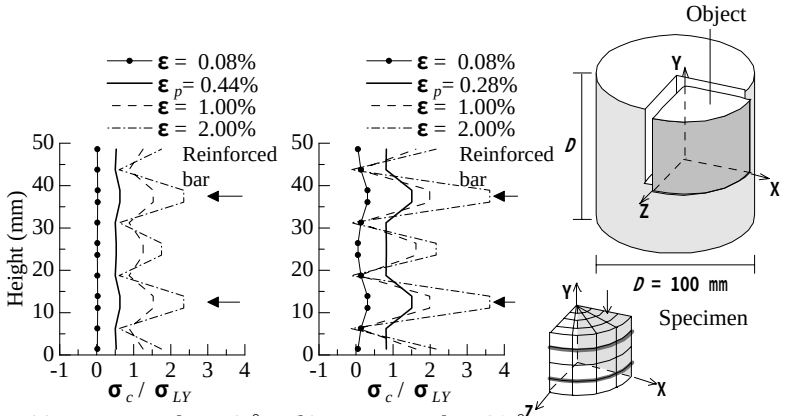

Figure 1 Distribution of equivalent lateral pressure σ_c (r = 49 mm, Reinforced bar : beam element, σ_{LY} =1.67 MPa)

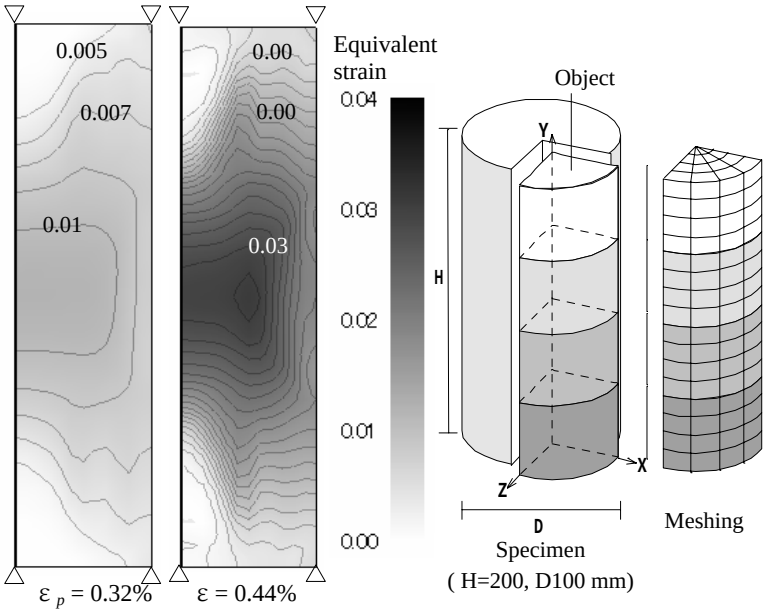

Figure 2 Distribution and progression of equivalent strain along height of column（φ= 53 deg.）

Mechanical Behavior of un-embedded Column Bases in Steel, CFT and SRC Structures

Haruyoshi Kadoya
(Building Structural System, Division of Systems Engineering)

Keywords: un-embedded column base, CFT, SRC, ultimate strength, rotational rigidity, elastic-plastic behavior

1. Introduction

1.1 Purpose

A survey report for damaged steel structures due to the great earthquake in the southern part of the Hyogo prefecture in 1995", made by the Society of Architecture in Japan, presents many cases of damaged un-embedded type column bases in steel structures including details of the damage on base plates, anchor bolts and foundation-concrete blocks that are components of un-embedded type column bases. The report states that those column bases must have been seriously damaged under action of extraordinary large axial forces in tension as well as in compression generated during the earthquake motion. This study aims to clarify the stress transfer mechanism on the un-embedded type column base, particularly when it undergoes large axial forces in tension, and proposes practical solutions to enhance the earthquake-resisting performance of the column base as to be capable for avoiding the rupture mode which leads to collapse of building structures as a whole.

1.2 Review to research works ever made in this concern

Research works ever made to evaluate the bearing strength of bare type steel column bases, CFT column bases, SRC column bases, and other concrete supports are reviewed as many as available and sorted out accordingly. However, it must be mentioned that very few of these studies addressed the load bearing mechanism and the reinforcing method for the column bases, particularly in case of the fixed type column bases under action of axial tensile forces.

2. Study on mechanical behavior of un-embedded and fixed type steel column base undergoing bending moments

Focusing attention to the out-of-plane bending deformation of the base plate and the behavior of the foundation concrete block undergoing compressive loads via the bottom surface of the base plate, the rigidity and ultimate resistance force of the column base are studied. For the above-mentioned study, experiments are carried out on the captioned column base. Applied experimental factor is the ratio of the resistance forces between the anchor bolts and the base plate. The results are compared with the structural behaviors of the column base obtained from FEM analysis. Various behaviors such as out-of-plane bending deformation of the base plate, elongation in the anchor bolts, and the foundation concrete block undergoing compressive loads via the bottom surface of the base plate are examined in detail. Consequently, the stress transfer mechanism in the column base can be made clear. Based on these findings, a set of design formula is proposed for evaluating rotational rigidity, yield strength load, and ultimate resistance force in the elastic region.

3. Study on mechanical behavior of un-embedded and fixed type column base undergoing bending moments coupled with constant axial forces (in tension/compression)

The structural behaviors of the un-embedded type column base are studied by carrying out a series of experiments and FEM analysis with use of full-scale test models of the column base under action of bending moments coupled with constant axial forces (in tension/compression). Under action of large axial forces in tension, elongations in the anchor bolts may cause pulling off the base plate. It is assumed accordingly that the effective area for the resultant compressive forces underlying the bottom surface of the base plate would decrease to result rupture in the concrete block. On the other hand, under action of large axial forces in compression, it can be assumed that the resultant compressive forces may cause bearing failure as the rupture mode of the foundation concrete block.

The test scheme is established to carry out for finding the resistance force of the column base using

Okabe Co., Ltd

full-scale test models of the column base with identical shapes and dimensions. Applied experimental factor is applying constant axial forces in tension or in compression. Another test scheme is established to carry out for bearing tests with local loading on the concrete block model to simulate bearing failure of the foundation concrete block in the column base. Based on these test results, a set of design formula is proposed for evaluating the resistance force of the column base.

4. Study on mechanical behavior of un-embedded type CFT column base

A new construction method is proposed to enhance the total integrity of all components in the un-embedded type CFT column base.

(1) An appropriate opening is made in the center of the base plate.
(2) The central reinforcing bars, embedded in the foundation concrete block in advance, are extended upwards into the steel column passing through the opening in the base plate.
(3) On completion of binding the base plate to the anchor bolts and erection of the column base, the space inside the steel column is filled with concrete to form a CFT column.
(4) Thus all the components in the CFT column and the foundation concrete block are tightly connected to form an integrated CFT column base.

The test scheme is established to carry out using full-scale test models of the CFT column of either a square or circular section steel tube with an RC structure base. Applied experimental factors in this case are (1) with or without the central reinforcing bars, (2) assigning different strength of the central reinforcing bars, and (3) applying constant or changing axial forces in tension or in compression. Based on both of the experimental results and the results from FEM analysis, the stress transfer mechanism and the characteristics of the hysteresis loops in the column base derived by incorporating the central reinforcing bars are examined. As a consequence, a set of design formula is proposed for evaluating rotational rigidity, yield strength load, and ultimate resistance force.

5. Study on mechanical behavior of un-embedded type SCR column bases

A new construction method is proposed to enhance the total integrity of all components in the un-embedded type SRC column base.

(1) An appropriate opening is made in the center of the base plate.
(2) The central reinforcing bars, embedded in the foundation concrete in advance, are extended upwards into the steel column passing through the opening in the base plate.
(3) On completion of binding the base plate to the anchor bolts and erection of the column base, surrounding RC structure is fabricated to form SRC column.
(4) Thus the SRC column base is formed as a fully integrated structure.

The test scheme is established to carry out using full-scale test models of the SRC column base. The amount of the main reinforcement bars in the surrounding RC fabrication is kept constant for all cases. Applied experimental factor in this case is assigning different quantity of the steel material (anchor bolts + central reinforcing bars) along the axial direction of the column base. The loading scheme is defined as bending moments coupled with the axial tensile forces applied to the column base. The design method of the SRC column base fabricated with the method proposed here, resultant yield strength load, and ultimate resistance force are examined. As a consequence, a set of design formula is proposed for evaluating rigidity, yield strength load, and ultimate resistance force of the SRC column base.

6. Conclusions

All the findings and consequences derived from this study are summarized. Finally, some remarks are made about the task ahead for further improvement to the un-embedded type column base.

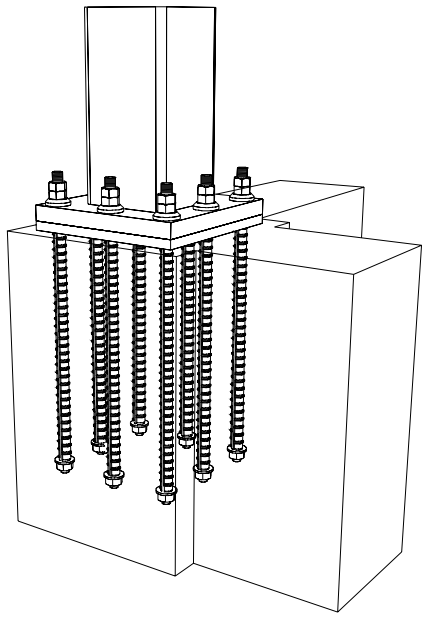

fig. Column Base Configuration

Studies on Surface Fusing, Globular Forming of Fine Solid Particles by a High Temperature Air Jet Flow

Hirokazu Nakamura †
(Fluid Engineering, Division of System Engineering)

Keywords : High temperature air jet flow, Flow and heat transfer, Fine solid particles, Gas-solid flow, Surface fusing, Globular forming

1. Introduction

High temperature air jets are used widely in the various fields of industry, such as heating, drying, powder treatment and others, but the heat transfer characteristics from high temperature air jet to fine particles have not been sufficiently understood yet.

In general, in order to produce powder/ particles of a few micro-meter the jet grinding method is used. Particle laden jet is made impinged on target plate, and then the particle is pulverized. The shape of grinded fine particle is not spherical nor uniform. In order to improve the efficiency of the powder, surface fusing or globular forming is required. Especially, the globular-formed color toner for copy machine will improve transcript efficiency and picture quality since electrification is uniform, durability and fluidity are improved.

The main purpose of this study is to improve the performance of surface fusing, or globular forming system of fine thermoplastic fine particles. First, the velocity and thermal characteristic of high temperature air jet from the around-nozzle and the new three-concentric-nozzle has been investigated experimentally, and the relation between the heat transfer from high temperature air jet to fine particles. Next, a globular forming characteristics has been investigated. The effect of nozzle shape on the performance of globular forming were also examined. As the result, in case of the globular forming performance, it shows that the new globular forming system has higher performance for toner I: approximately 5.4 times greater energy efficiency compared with the former one.

2. Experiment and Results

Figure 1 shows the former and new globular forming systems, called the around-nozzle (a) and the three-concentric-nozzle (b), respectively. For the three-concentric-nozzle, in order to create the flow and temperature fields in which all particles pass through the high temperature region, the raw material is injected by the sub nozzle which is placed at the center of the main nozzle. The relation between the heat transfer rate to fine particle and globular forming characteristics is investigated experimentally. The flow and heat transfer characteristics is investigated by flow visualization with a thermograph. The evaluation of energy efficiency for globular forming with the new three-concentric-nozzle is understood by forming globular for a few materials.

Figure 2 shows the relation between the mean roundness and heat transfer rate to a fine particle of d_p=8.8μm. The mean roundness is improved by increasing heat transfer rate to fine particle.

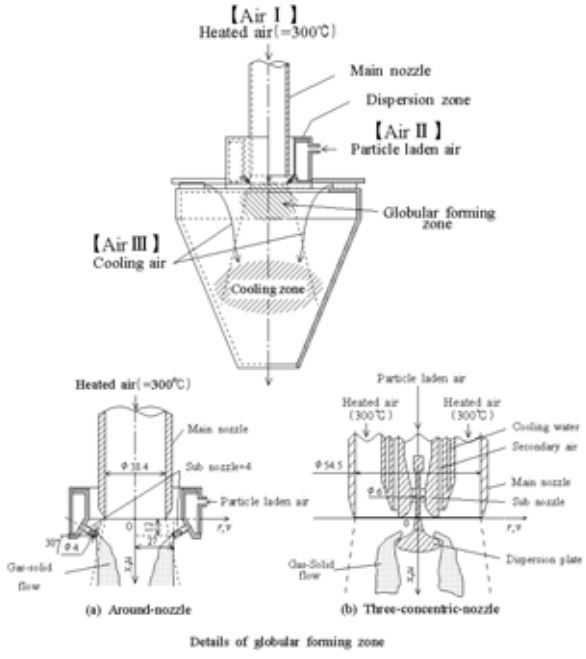

Fig.1 Globular forming systems

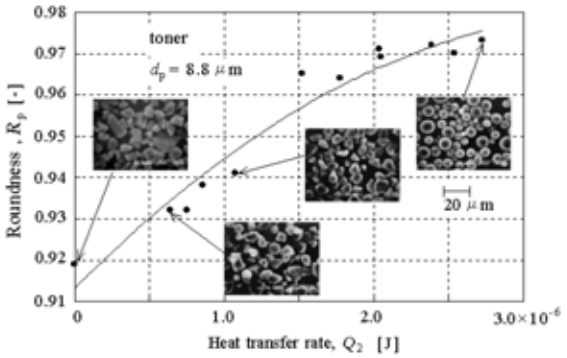

Fig.2 Roundness and heat transfer rate to fine particle

† Nippon Pneumatic MFG. CO., LTD

Figure 3 and 4 show the temperature profiles of high temperature air jet flow for the around-nozzle and the three-concentric-nozzle, respectively. In Figures 3 and 4, the sketches of fine particle's flying trajectories in the high temperature field are also shown. It is confirmed that the three-concentric- nozzle can introduce most of the particles to the high temperature region of T>200°C, comparing with the around-nozzle. In case of the globular forming performance, the energy efficiency ratio of the new globular forming system for toner I (d_p50=8.8μm) and II (d_p50=7.4μm) are considerably improved to about 5.4, 3.2 times, respectively, comparing with the former one and the around-nozzle.

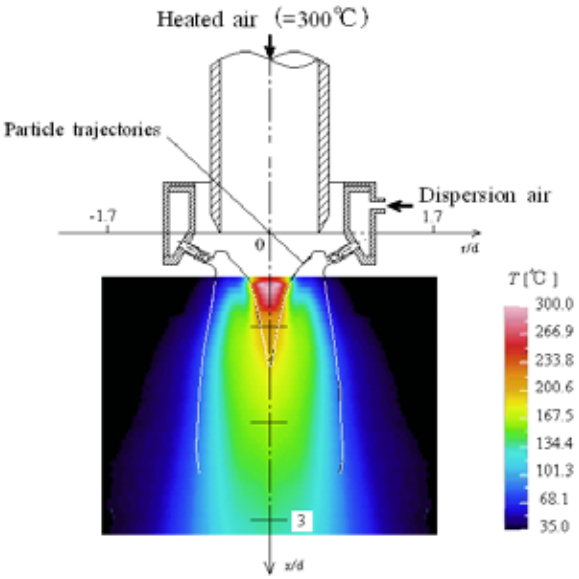

Fig.3 Temperature distribution and particle trajectories of around-nozzle

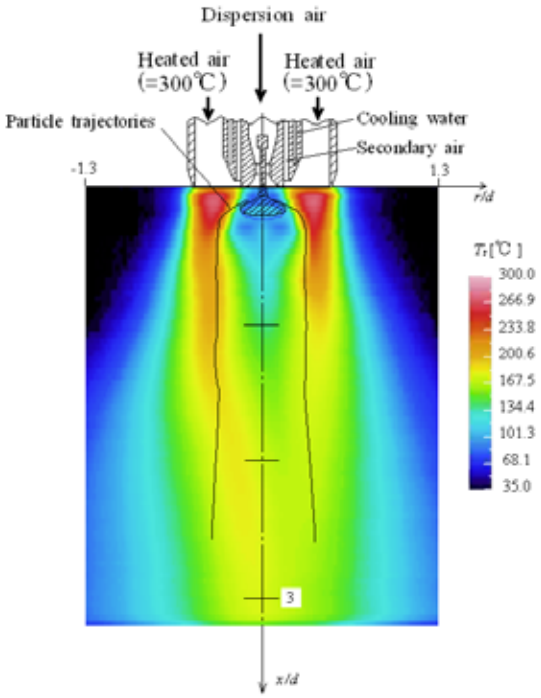

Fig.4 Temperature distribution and particle trajectories of three-concentric-nozzle

3. Concluding remarks

A new globular forming system, the three-concentric- nozzle, was proposed, and the globular forming performance was clarified by heat transfer characteristic to a fine particle, visualization of particle flying trajectory and others.

i) The most particle is introduced into the high temperature region of T>200°C in the case of the three-concentric-nozzle, comparing with the around-nozzle.
ii) The relations between the heat transfer rate to fine particle Q_2 and mean roundness R_p were clarified, and R_p increases with increaseing Q_2. These relations can be expressed by
$R_p=(-4.84\times10^9)Q_2{}^2+36000Q_2+0.91$
iii) The mean roundness R_p and coupling Δd_p for the three-concentric-nozzle are considerably improved comparing with that for the around-nozzle in the case of the same feed rate G.
iv) The energy efficiency ratio of the new globular forming system for toner I and II are considerably improved to about 5.4, 3.2 times, respectively, comparing with the former one and the around-nozzle.

Author's publications

[1] Shakouchi, T., H. Nakamura, A. Kusuda, D. Sakamoto and M. Okumoto, *Flow and Heat Characteristics of High Temperature Round Jet*, Proc. of JSME, No.033-1, pp.63-64, Mar.,2003
[2] Shakouchi, T., Nakamura, H., Morimoto, H., Okumoto, M., *Flow and Heat Transfer of High Temperature Circular Jet and it' Application*, Proc. of JSME, No.03-30, pp.283-284,Nov.,2003
[3] Nakamura, H., Shakouchi, T., Kusuda, A., *High Temperature Air Jet Flow and Its Application to Globular Forming of Fine Particles*, Trans. of SCEJ, No.6, pp.836-841, Nov.,2003
[4] Nakamura, H., Shakouchi, T., *A New Surface Fusing, Globular Forming Method of Fine Particle*, Trans. of JSME, 70-699 B, pp.255-262,Nov.,2004
[5] Hirokazu Nakamura, Toshihiko Shakouchi, *Flow and Heat Control of High Temperature Air jet and Application to Surface fusing of Fine Particle*, Proc. of 5th Internatinal Conference on Multiphase Flow, CD-ROM, Jun.,2004

Study on sound insulation of absorptive louver

Toshio Matsumoto †
(Information and communication systems, Division of Systems Engineering)

Keywords: Absorptive louver, Insertion loss, Sound reduction index, Road traffic noise, Semi-underground road, Noise barrier

1. Introduction

Absorptive louvers have been developed as facilities for road traffic noise control at semi-underground roads and road tunnel entrances. So far, a total surface area of about 50,000 m^2 of the absorptive louvers has been installed along express ways. The noise reduction of the absorptive louvers greater than 10 dB has already been obtained for A-weighted road traffic noise. However several problems have been remained in the determination of effectiveness as a sound insulation of the absorptive louver. The sound insulation of the absorptive louvers has been examined by full-scale experiments and evaluated by insertion loss. However, insertion loss is not an intrinsic quantity, and then measurement and evaluation methods are not standardized. Furthermore, the prediction of the efficiency of the absorptive louvers has been important in the promotion of urban planning and environmental impact assessment. Structure factors affecting sound insulation of absorptive louver are not investigated in detail. It shall be expected that the field of its application expands. Therefore measurement, rating and prediction methods of sound insulation of absorptive louvers are required. On the other hand, highway noise barriers are required not only to reduce noise, but also to improve a view, taking account of recycling material and reduce costs in recent years. In order to comply with the request, absorptive louver blades are applied to barriers.

In this study, measurement, rating and prediction methods of sound insulation of absorptive louvers are investigated. Furthermore, new type highway barriers are developed, which are applied to functions of absorptive louvers.

2. Absorptive louvers

The absorptive louvers have been developed in Japan, in which three functions of noise reduction, lighting and ventilation control are combined. The louver was originally designed as lighting control systems for entrances of highway tunnels. In order to reduce noise, the louver blades are treated with absorptive material. The original louver consists of panels bent at angle of 120 degrees, and the panels are called louver blades. Each blade is made of glass wool with a thickness of 100 mm, a thin film of polyvinyl fluoride (PVF) for waterproofing and a stainless steel box with perforated facings. The thickness of the blade is 105 mm and the width is 580 mm. The louver blades are arranged within a frame, with the blades equally spaced apart, so that the direct incidence of sunlight into the roadway may be avoided. Figure 1 shows an example and a cross sectional view of an absorptive louver.

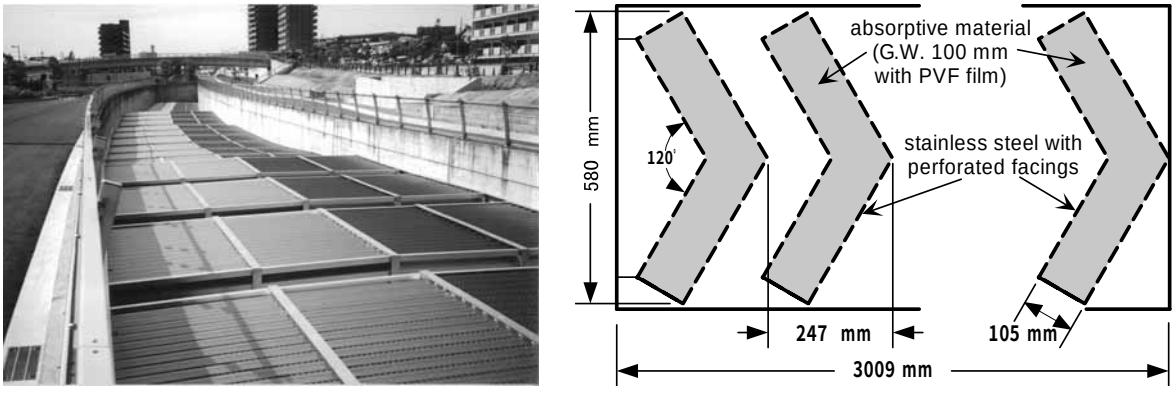

Fig. 1 An example and a cross sectional view of an absorptive louver.

† Kobayasi Institute of Physical Research

3. Measurement and rating of sound insulation of absorptive louvers

In order to measure and evaluate the sound insulation of the absorptive louvers, the insertion loss and sound reduction index of the louver are studied. The relationship between the indices is formulated based on geometrical acoustics, in the case where the louver is set up at an opening between a diffuse sound field and a free sound field. In verifying the equation, trial products of the louver are produced in full-scale, and then the experiments are carried out by setting up a louver at the opening of a reverberation room. Insertion loss IL is determined from the mean value of the level difference with and without the louver. Sound reduction index R_I was measured by sound intensity technique (ISO 15186-1). This result shows that the theoretical expression of the relationship between insertion loss and sound reduction index is appropriate. Furthermore, insertion loss of the absorptive louver for the semi-underground roads is calculated, and compared with the data of in-situ and laboratory measurements. The calculated and measured results of insertion loss for A-weighted road traffic noise are in good agreement. This result shows that insertion loss of the calculated data and the measured data can be evaluated for the sound insulation of the absorptive louvers.

4. Prediction of sound insulation of absorptive louvers

The prediction of the insertion loss of the absorptive louvers has been investigated by using full-scale model experiment and two-dimensional boundary element method (BEM). Structure factors affecting sound insulation of the absorptive louvers, which are considered in the experiment and numerical analysis, are as the following: the total absorptive area per unit area of the louver, absorptive coefficient and the spacing of the blade.

Expressions of the relationship between these factors and insertion loss for A-weighted road traffic noise are obtained from the test results. In the numerical simulation, the calculated value is greater than the measured value in all frequencies. The frequency characteristics of the calculated data, however, are the same as that of the measured data in shape. This result shows that the numerical simulation by BEM can apply to relative evaluation of insertion loss of the absorptive louver.

5. Development of highway noise barrier with horizontal louver

A type of highway noise barrier is designed to possess both acoustical and non acoustical benefits such as amenity for residents and drivers. In the design, absorptive louver blades are applied to barriers so that the acoustical performance of the barrier can be improved. The barrier, i.e., horizontal louver, looks like sun shading blinds.

The acoustical performance of this type is examined by 1/5 scale model experiments and calculated by two-dimensional BEM. Trial products of horizontal louver are made in full scale and the efficiency of barriers to the highway noise is investigated at a place where an elevated road is simulated. Test results show that noise reduction of 2 dB over conventional barrier is obtained.

Furthermore, in the case of miniaturization of the absorptive louver blades, the efficiency of noise barrier with horizontal louver has been studied by using BEM. Sound pressure levels at the area behind the barrier are greater than the reference wall. This increase is caused by the sound leakage through the apertures of the barrier, so that the absorptive coefficient of the small-sized blades is lower than that of the normal-sized one. It becomes clear that applying high absorptive material to the blade surface is favorable to the improvement of the efficiency of the barrier with horizontal louver.

6. Conclusions

The measurement and the rating of the sound insulation of the absorptive louvers are investigated. This result shows that insertion loss can be measured and evaluated for the sound insulation of the absorptive louvers. The insertion loss of the absorptive louvers can be predicted by combining full-scale model experiment and two-dimensional boundary element method (BEM). Furthermore, highway noise barrier with horizontal louver are developed, in which absorptive louver blades are applied to barriers. The test results show that the additional attenuation greater than 2 dB can be obtained.

The application of the absorptive louver and the highway noise barrier with horizontal louver may help to solve the various environmental problems.

Author's publications

[1] T. Matsumoto, R. Hotta and K. Yamamoto, "Efficiency of highway noise barrier with horizontal louver", The Journal of the INCE of Japan, Vol.26, No.2, pp.129-137, 2002. [in Japanese]

[2] T. Matsumoto, K. Yamamoto and K. Kuno, "Measurement and rating of sound insulation of absorptive louver", The Journal of the Acoustical Society of Japan, Vol.60, No.11, pp.646-654, 2004. [in Japanese]

Improvement of machinability of Aramid fiber reinforced plastics and clarification of the behaviors of fibers during machining

Eitoku NAKANISHI

Keywords: Aramid fiber, Composite materials, In-situ observation, Ultrasonic vibration, Oblique cutting, Fiber orientation, Beam theory,

1. INTRODUCTION

Recently, the composite materials are used very widely. However, the machining of composite materials is very difficult due to the much differences of mechanical properties between the reinforcing materials and matrix materials. Especially the machining of an Aramid fiber reinforcing plastics (A-FRP) causes the rough machined surfaces. And we chose Aramid fiber as reinforcing material and unsaturated polyester (UP) as matrix material. The surface integrities are much affected by orientation of fibers and machining conditions. Therefore, we try to establish the optimum method for machining the A-FRP. To clarify the effect of fiber orientation on the surface appearances, we carried out in-situ observation of deformation and fractural phenomena of Aramid fiber during machining A-FRP. And we proposed simple models to evaluate the deformation of Aramid fiber bundle and fracture point of Aramid fiber during machining. Furthermore, we proposed some unique and effective methods for machining the A-FRP in high surface quality.

2. EXPERIMENTAL

To observe the behaviors of Aramid fiber bundle during machining, we carried out in-situ observation as shown in Fig.1. The Aramid fibers are situated inside of the matrix material, so the fibers are observed transparently through the matrix material by using optical microscope. When fiber angle θ is 45 degree, cutting tool lifts up the Aramid fiber and bends the Aramid fibers towards the cutting direction. With advances of the cutting tool, the large delamitation between Aramid fiber and matrix can be observed inside of the matrix. And after the tool passed, large fluffs appear on machined surface. In this case, the machining surface integrities become very poor. On the other hand, when fiber angle θ is 135 degree, only the Aramid fibers, which exist near the cutting tool edge, are deformed along the cutting tool edge radius. And after the tool passed, no fluffs and no delamination appeared on machined surface and the surface integrities becomes well. Further to clarify the relationships between the radius of cutting tool edge and fracture behavior of Aramid fiber, we cut Aramid fibers in SEM chamber by using special equipment. When the tool edge is dull, Aramid fibers are cut with fibrillating and hang together.

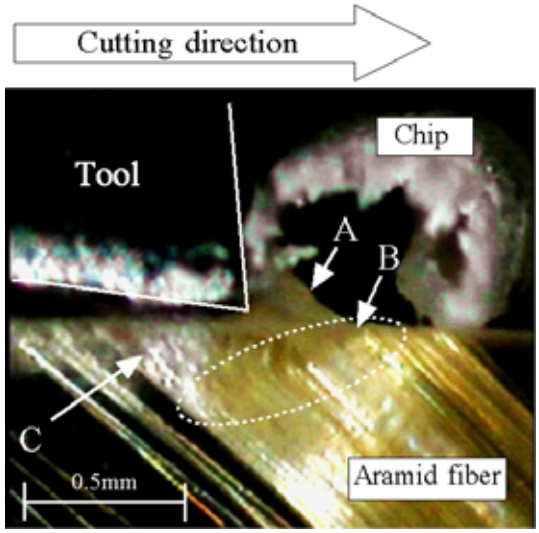

Fig.1 Deformation of Aramid fiber bundle

3. SIMULATIONS

We proposed two types of simulation models. The first model is based on the beam theory, in which the beams are regarded as Aramid fiber bundle and the elastic foundation is regarded as matrix material to depict fiber bundle deformation in each fiber orientations. The second model is to describe the stress distribution for evaluating the fiber fracturing point to consider the fluff length that appears on machined surface. For more accurately describing, the bonding strength and frictional coefficient between the Aramid fiber and UP in experimentally, and these values are introduced into the present model.

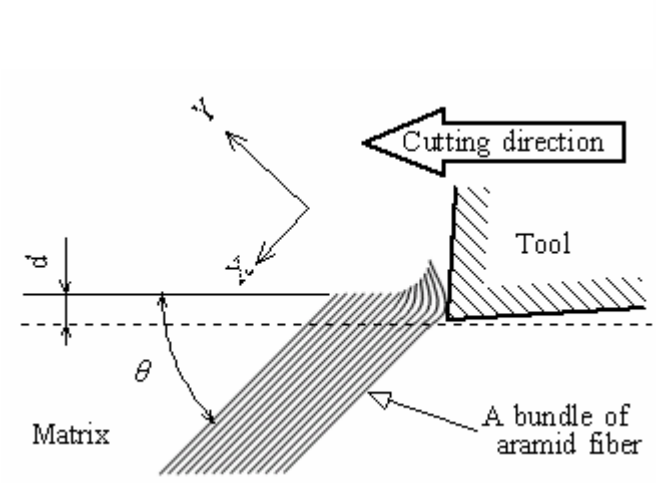

Fig.2 Model based on the beam theory

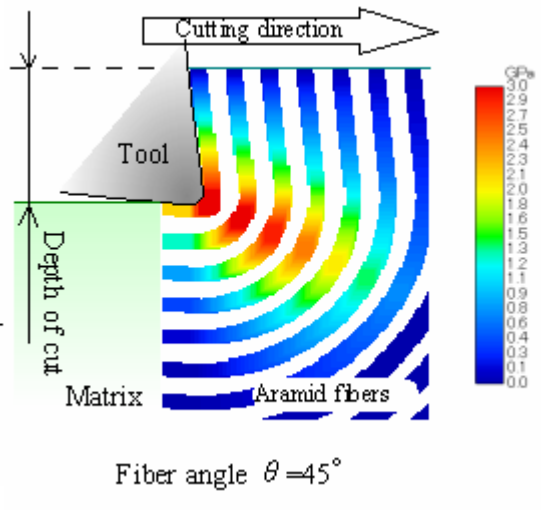

Fig.3 Stress distribution

4. PROPOSED MACHINING METHOD

We proposed two types of machining method. One is cutting with ultrasonic vibration and the other is oblique cutting. When the frequency is 20KHz and amplitude is 15μm, the critical cutting speed becomes 84 m/min during cutting with ultrasonic vibration. If the cutting speed is slower than critical cutting speed, it may become very effective because of interrupted cutting and the change of cutting velocity in continuously. When applying the cutting with ultrasonic vibration to machining the A-FRP, the tool wear progress was reduced than normal type of cutting and the tool edge radius was kept sharp in long cutting distance. And the machined surface integrities kept high quality in long cutting distance. Surface roughness becomes very small and very smooth machined surface can be obtained during oblique cutting.

5. CONCLUSONS

In the present thesis, the fracture phenomena of Aramid fiber can be observed clearly by in-situ observation. And our simulations show a good coincident with observation result. Further, the proposed machining method shows high performance for applying to A-FRP. These results show possibilities of machining the A-FRP materials in higher quality and contribution to spreading field of use the A-FRP materials.

Author's publications

- A.K.M. MASUD, Eitoku NAKANISHI, Jippei SUZUKI and Kiyoshi ISOGIMI, Cutting phenomena of Aramid-glass Hybrid FRP with Ultrasonic Vibration, Post Conf. Proc. of the 8th International Congress on Experimental Mechanics (SEM), pp.111-116 (1996).
- Eitoku NAKANISHI, Jippei SUZUKI and Kiyoshi ISOGIMI, Effect of Vibrations on Fracture Phenomena in Machining Aramid-Glass Fiber Hybrid Composites, Engineering Transactions, Vol.47, No.2, pp.145-154 (1999).
- Eitoku NAKANISHI and Kiyoshi ISOGIMI, Fracture Phenomena of Aramid Fiber during Oblique Cutting, Proc. of 10th International Conference on Precision Engineering (ICPE), pp.259-263 (2001).
- Eitoku NAKANISHI, Yutaka SAWAKI and Kiyoshi ISOGIMI, Microscopic Observation of Fiber Deformation and Fracture During Machining A-FRP, FACTA UNIVERSITATIS, Series: Mechanics, Automatic Control and Robotics, Vol.3, No.13, pp.739 –744 (2003).
- E. NAKANISHI, Y. SAWAKI and K. ISOGIMI, Modeling of Deformation of Aramid Fiber Bundle During Machining Aramid FRP (in Japanese), Journal of Japan Society of Advanced Production Technology, Vol.22, No.1, 67-74 (2004).